UNIVERSITY OF CAPE TOWN
FACULTY OF ENGINEERING AND THE BUILT ENVIRONMENT

A comparison of the least squares collocation and the fast Fourier transform methods for gravimetric geoid determination.

Author: Siphiwe M. Mphuthi

Supervisor: Dr Ramesh Govind

May 2016

The School of Architecture, Planning and Geomatics

Research project prepared in partial fulfilment of the requirements for the Degree:

MSc. (Eng.) in Geomatics

PLAGIARISM DECLARATION

NAME: SIPHIWE M. MPHUTHI **STUDENT ID: MPHMAT021**

1. I hereby declare that I know what plagiarism entails, namely to use another's work and to present it as my own without attributing the sources in the correct way.
2. I know that plagiarism is a punishable offence because it constitutes theft.
3. I understand the plagiarism policy of Faculty of Engineering and the Build Environment of the University of Cape Town.
4. I declare therefore that all work presented by me for every aspect of my thesis, will be my own, and where I have made use of another's work, I will attribute the source in the correct way.

Signed by candidate

Signature: _____ Date: ____03-10-2016_____

Acknowledgements

First and foremost, I'm heartily grateful to my supervisor Dr Ramesh Govind, for his encouragement, support and guidance provided from the beginning to the end of the project. I am indebted to his valuable comments, professional advice and assistance through the process of developing the idea for this research and making it reality.

I would like to express my deep gratitude to the Department of Rural Development and Land Reform for the financial support they provided for my studies, this research wouldn't be initiated and completed without their support.

I would like to thank the National Geo-Spatial Information (NGI), for providing data (GPS/Levelling and gravity data) for this research. This research could not be completed without this support, this support is cordially acknowledged.

I'm indebted to all the staff and lecturers from the department of Geomatics for all the assistance provided to help me complete this research, Dr G Sithole, A/Prof. J Smit, Prof. H Ruther, A/Prof. J Whittal, Mr S Hull, Ms M Wells and Mr D Matthee. I would like to extend my thanks to the other post graduate students I shared an office with, Ms Naa Dedei Tagoe, Mr Almabrok Uheda, Ms Mobless Shoko and Mr Matthew Westaway.

I would like to greatly extend my thanks to my friends in the department of Geomatics, UCT, Sifiso Mthembu, Thabo Ntsoko, Masixole Bantom and Luvo Qumba for their assistance through all difficulties; and emotional support, camaraderie, entertainment, and caring they provided.

I owe my deepest gratitude to my parents, siblings and lovely partner Nokwazi P. Nkosi for all their support, patience and encouragement. I would like to expand my thanks to the Lord above for making it possible for me to make it this far.

University of Cape Town, May 2016

Siphiwe M. Mphuthi

TABLE OF CONTENTS

LIST OF FIGURES

LIST OF TABLES

LIST OF NOTATIONS

SYMBOL	DESCRIPTION	UNITS
GM_g	mass gravity constant of the geopotential model	$m^3 s^{-2}$
a_g	semi-major axis of the geopotential model	meters
GM	mass gravity constant of the reference ellipsoid	$m^3 s^{-2}$
a	semi-major axis of the reference ellipsoid	meters
f	flattening parameter of the reference ellipsoid	no units
b	semi-minor axis of the reference ellipsoid	meters
E	linear eccentricity	meters
e	first (numerical) eccentricity	no units
e'	second (numerical) eccentricity	no units
ω	angular velocity of the Earth's rotation	s^{-1}
λ	longitude	degrees or radians
φ	geographic latitude	degrees or radians
$\bar{\varphi}$	geocentric latitude	degrees or radians
r	local elliptic radius	meters
$\bar{g}$	mean gravity	ms^{-2}
γ	local normal gravity	ms^{-2}
γ_a, γ_b	normal gravity at the equator and at the poles	ms^{-2}
$\bar{C}_{n,m}, \bar{S}_{n,m}$	fully normalized spherical harmonic coefficients	no units
	(or Stokes' coefficients) of the gravity model	no units
$P_{n,m}$	associated Legendre functions of the first kind	no units
$\bar{P}_{n,m}$	fully normalized harmonics	no units

ABSTRACT

The objective of the research was to study the performance of the least squares collocation (LSC) and the fast Fourier transform (FFT) techniques for gravimetric geoid computation.

The Land Levelling Datum (LLD) is the South African vertical datum based on more than 100 years old tide gauge measurements of mean sea level (MSL). The LLD is poorly defined so an alternative is required. The SAGEOID10 (Merry, 2009) hybrid geoid model was computed for the purpose of replacing the existing vertical datum.

Two gravimetric geoid models were computed using different techniques for evaluation of the Stokes' integral, such as, LSC and one dimensional fast Fourier transform (1D-FFT) technique. The long wavelength component of the geoid models were computed using the EGM2008 geopotential model truncated at degree 720.

The use of fast spectral techniques is required due to an increase of both quality and type of data available for geoid determination. The FFT method is most reliable than the LSC method, since it requires less computational time on large data set than the LSC. A system of linear equations of order equal to the number of data points is generated on the LSC method.

The geoid model was computed over the province of Gauteng. It was then compared to the SAGEOID10 hybrid geoid model. The computed geoid models, SiPLSC and SiPFFT geoid model compared to the SAGEOID10 model with standard deviation of 5.6cm. The long wavelength component of the computed geoid model compared to the EGM2008 geopotential geoid model with a standard deviation of 4.2cm.

1 INTRODUCTION

The geoid, by its definition as the equipotential surface of the earth's gravity field which on average coincides with the undisturbed Mean Sea Level (MSL), provides the appropriate reference surface for heights. Therefore, traditionally, national and regional height datums were defined with respect to a selected network of tide gauges; and height networks were established by terrestrial techniques such as spirit levelling.

The South African vertical datum, generally referred to as the Land Levelling Datum (LLD) or Primary Levelling Network, and classified as a spheroidal orthometric height system, is based on the determined mean sea level from tide gauge observations (since early 1900's) at Cape Town, Durban, East London and Port Elizabeth (NGI 2013, Wonnacott and Merry 2012). Although Wonnacott and Merry (2012) state that the period of tide gauge observations for determining MSL at these tide gauges was rather short (1-2 years), no exact information on the length of tide gauge observations is available.

The accelerating growth in the use of the Global Navigation Satellite System (GNSS), such as the Global Positioning System (GPS), GLONASS, Galileo, Beido/Compass, Indian Regional Satellite System (IRNSS)/Navigation with Indian Costellation (NavIC) for 3-Dimensional positioning has intensified the requirement for geoid heights that are consistent with the attainable accuracy of the ellipsoidal heights that are determined from GNSS. It is for this transformation, from ellipsoidal heights to MSL heights that an accurate geoid is required. The relationship between the ellipsoidal (h), orthometric (H) and geoidal heights (N) is shown in figure (1-1) and equation 1.1 below.

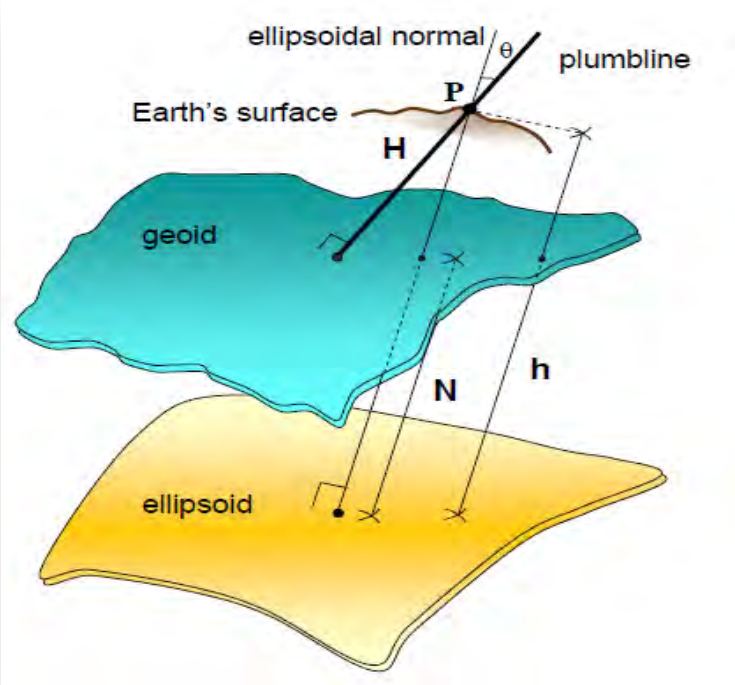

Figure 1-1: Relationship between ellipsoidal height (h), orthometric height (MSL, H) and geoid height N (Sideris, 2013)

$$N = h - H \tag{1:1}$$

The development and availability of global geopotential models derived from satellite and terrestrial gravity data has led to significant improvement in the accuracy and resolution of global geoids. These models (Table 1-1 below) emanate from recent dedicated gravity missions such as the Gravity Recovery and Climate Experiment (GRACE), and Gravity field and steady state Ocean Circulation Explorer (GOCE). In addition, there has been an increase in the number of satellite altimetry missions such as TOPEX-Poseidon, Jason-1, Jason-2, Envisat and the ERS missions that further contributed to the improvement of the geopotential models describing the global geoid.

This has also been further enhanced by the combination of satellite tracking data. There has been a significant increase in satellite tracking data such as Satellite Laser Ranging (SLR), Doppler Orbitography Range Inferred from Satellite (DORIS) and GPS Low Earth Orbiting Satellites (LEOs). Which when combined with the GRACE Ku-band satellite-to-satellite tracking and the GOCE gravity gradiometry data has provided estimates of the spherical

harmonic coefficients, describing the geopotential model, at high resolution and with unsurpassed accuracies. A sample of recent global geopotential models are listed below on table 1-1.

Table 1-1: Global geopotential models

Model	Year	degree	Data Type	Reference
EGM96	1996	360	Satellite(SLR, Altimetry), Terrestrial Gravity	Lemoine et al, 1998
EIGEN-CG03C	2005	360	CHAMP, GRACE, Terrestrial Gravity, Altimetry	Föreste et al, 2005
EGM2008	2008	2190	GRACE, Terrestrial Gravity, Altimetry	Pavlis et al, 2008
EIGEN-6C4	2014	2190	GRACE, GOCE, SLR, Terrestrial Gravity, Altimetry	Föreste et al, 2014
GECO	2015	2190	GOCE + (EGM2008)	Gilardoni et al, 2016
GOCO 05c	2015	720	GRACE, GOCE, SLR, Terrestrial Gravity, Altimetry	Fecher et al, 2015

The resolution $(R = (2\pi * Earth\ Radius)/degree))$ of the geoid has improved from 110Km (for degree 360) to 18 Km (for degree 2190). Although there has been an improvement in the accuracy and resolution of global geopotential models, and satellite altimetry data, the volume and density of the observed terrestrial gravity data over South Africa remains constant.

However, the computational techniques for evaluating Stokes' integral (for the inner zone contribution) using gravity anomalies derived from the observed terrestrial data has improved, in particular for computational efficiency. The traditional numerical integration is replaced with fast Fourier transform (FFT) and least squares collocation (LSC) techniques.

The improved data sets (geopotential models) and computation techniques provide an opportunity to compute a geoid model over South Africa. To attain geoidal heights and hence orthometric heights at accuracies that are consistent with GNSS determined ellipsoidal heights; and MSL heights that are compatible with South Africa's LLD. This overcomes

some of the disadvantages of spirit levelling – labour intensive, expensive, access to remote and mountainous areas.

Several national agencies around the world such as Australia (Featherstone et al 2011), Canada (Huang and Véronneau 2013, Natural Resources Canada 2013), Europe (Denker et al 2009), New Zealand (Amos, 2010; Land Information New Zealand, 2015) South American countries (Blitzkow et al, 2012 and Guimarães, 2012)and the United States of America (Roman et al, 2009, Zilkoski, 2015, NGS 2015) have embarked on recomputing/redefining their vertical datums; evolving into a geoid based height system.

In recent times, a continental geoid for Africa, three versions of a regional geoid for Southern Africa and a national geoid for South Africa have been modelled. These are introduced below and further discussed in sections 1.1, 1.2 and 1.3.

The African Geoid Project of 2003 (AGP2003), developed by Merry *et al.(* 2003) is a quasi geoid model which was developed for the purpose of having a unified precise vertical datum for Africa to provide support of infrastructure and development across the continent.

Three UCT quasi-geoid models were computed for Southern Africa, namely, UCT2003 UCT2004 and UCT2006 (Merry, 2007).

The SAGEOID10 is the South African hybrid geoid which was developed for transforming GPS derived ellipsoidal heights to orthometric heights on the LLD. The precise hybrid geoid model SAGEOID10 was developed for the Chief Directorate: National Geospatial Information (CD: NGI) (Chandler and Merry, 2010).

1.1 **The African Geoid Project (AGP2003)**

The AGP2003 quasi-geoid model ζ is computed from a combination of four components, such as, long wavelength ζ_L, short wavelength ζ_S, the contribution from Molodensky G1 term ζ_{G1}, and innermost zone ζ_I (Merry et al, 2003).

The ζ_L of the AGP2003 quasi geoid model was computed from the Global gravitational model (GGM) EGM96 (Lemoine et al, 1998) complete to degree and order 360. The ζ_S was computed using the two dimensional convolution of the reduced gravity anomaly with Stokes function. The GLOBE digital elevation model was used to compute the terrain effect also

known as the Molodensky term (G_1). The ζ_I was computed from a linear approximation of gravity anomaly in the innermost small circle using reduced gravity anomaly grid spacing around the computational point.

The AGP2003 was validated using GPS/levelling data from different regions over Africa. The AGP2003 quasi geoid model was only validated over three regions namely Algeria, Egypt and South Africa. As illustrated by the table (1-1) below (Merry, 2003):

Table 1-2: Comparison GPS/levelling - AGP2003

Region	No. Points	Bias (cm)	Standard Dev. (cm)
Algeria	13	-17	48
Egypt	8	+124	80
South Africa	42	-63	9

The APG2003 height anomalies, when compared with 42 GPS/levelling data points over South Africa showed a bias of -63cm and standard deviation of 9cm. The AGP2003 quasi geoid model was compared with 13 GPS/levelling data points in Algeria bias of -17cm with a standard deviation of 48cm. It was finally compared with 8 GPS/levelling data points in Egypt showed a bias of +124cm with a standard deviation of 80 cm (Merry, 2003).

1.2 The UCT2006 quasi geoid models for Southern Africa

The UCT2006 quasi-geoid model is computed in the similar manner as the AGP2003 quasi-geoid model, described above. The long wavelength was computed from the EIGEN-CG03C model (Förste et al, 2005), complete to degree and order 120.

The short wavelength was computed using the residual gravity anomalies with the Stokes' integral. The Stokes' integral was evaluated using two dimensional fast Fourier transform method (Merry, 2007).

The contribution of the Molodensky G_1 term was computed from two different digital elevations models. The CDSM DEM (Merry, 2007) was used for South Africa and the SRTM30 model (Merry, 2007) was used for the remaining countries in Southern Africa.

The inner zone component uses a linear approximation for the gravity anomaly field in the innermost zone. It is the block of $\Delta\varphi\ by\ \Delta\lambda$ centred on the computational point.

The UCT2006 quasi-geoid model was validated using 62 GPS/levelling data points on the western side of South Africa. The comparison between the UCT2006 and geoidal height derived from the 62 GPS/levelling data points gave a standard deviation of 15cm (Merry, 2007).

Furthermore, this agreement can be improved by removing tilts and biases from the GPS/levelling measurements. The standard deviation was then reduced to 13cm (Merry, 2007). The quality and distribution of the available gravity data can still be improved, and more GPS/levelling data points are required for validation of the quasi geoid model (Merry, 2007).

1.3 South African geoid model (SAGEOID10)

The SAGEOID10 is the South African hybrid geoid model was computed from GPS/levelling data and combined with the gravimetric geoid model. The gravimetric geoid model was computed as follows (Chandler and Merry, 2010):

i. The long wavelength component was computed from EGM2008 (Pavlis et al, 2008) geopotential model complete to degree and order 360.
ii. The contribution of the short wavelength component (N_S) is computed using both land and marine gravity anomalies, together with a terrain correction.

The geometric geoid model was computed using 79 benchmarks distributed throughout the country. The geoidal height (N) of the geometric geoid model is computed from the difference between the ellipsoidal height (h), and the orthometric height (H) as expressed by equation (1:1) (Chandler and Merry, 2010).

The WGS84 ellipsoid was used as the reference ellipsoid during the computation of the SAGEOID10 hybrid geoid model. A correction surface is computed from the comparison of the geometric geoid model and the gravimetric geoid model. The correction surface is applied to the gravimetric geoid model to remove biases and tilts on the gravimetric geoid model.

The gravimetric geoid model is converted to a hybrid geoid model consistent with the GPS/levelling data using the correction surface (Chandler and Merry, 2010). The 79 GPS/levelling precisely measured data points from the 118 GPS/levelling data points were used for the development of the SAGEOID10 hybrid geoid model. The remaining 39 GPS/levelling points were used for the validation of the SAGEOID10 hybrid geoid model. The standard deviation of the SAGEOID10 hybrid geoid model was determined to be 7cm at the 39 GPS/levelling validation points (Chandler and Merry, 2010). The figure (1-2) below depicts the shape of the South African geoid model in contour form.

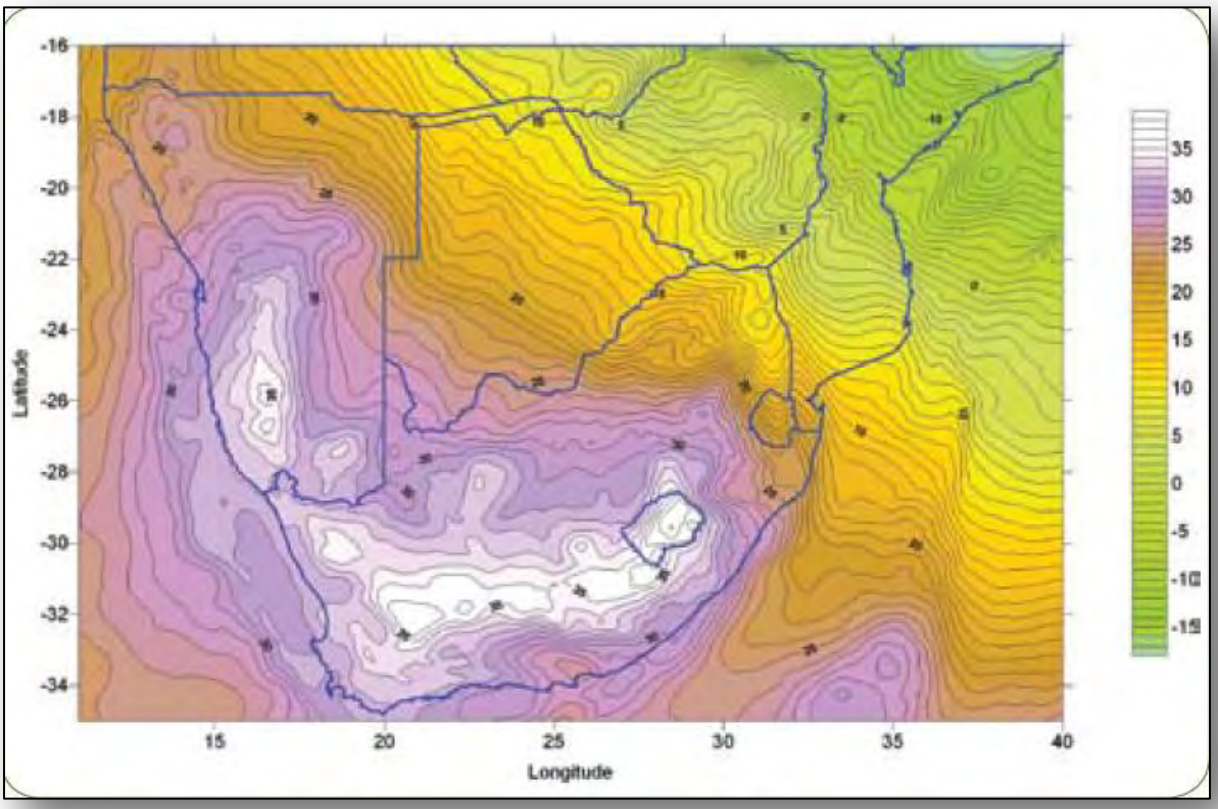

Figure 1-2: South African gravimetric model (SAGEOID10) (Chandler and Merry, 2010)

1.4 New Zealand Vertical Datum 2009

The New Zealand Vertical Datum 2009 (NZVD2009) was developed to unify the 13 separate existing Local Vertical Datums (LVDs). NZVD2009 is an official vertical datum for New Zealand (Amos, 2010).

The NZVD2009 uses the national geoid of New Zealand, the New Zealand gravimetric quasi geoid model 2009 (NZGeoid2009). The NZGeoid2009 model was computed using improved computational strategy and more data input (Amos, 2010).

New Zealand is the first country to implement the use of the geoid based vertical datum (NZVD2009). This provided New Zealand with the unified vertical datum, and better use of the GNSS technology within the country (Amos, 2010).

The long wavelength component was computed from the harmonic coefficients of the EGM2008 geopotential model complete to degree and order 2160. The short wavelength component was computed from the residual mean gravity anomalies. The residual mean gravity anomalies are computed from subtracting the gravity anomalies generated by the harmonic coefficients of the EGM2008 (Pavlis et al, 2008) geopotential model from the merged land and marine gravity anomalies (Claessens et al., 2009).

The NZGeoid2009 gravimetric quasi geoid model was validated using 1422 GPS/levelling data points that are spread among the 13 LVDs. It compared with an average standard deviation of $6.2cm$ (Amos, 2010).

New Zealand is the first country to implement the use of the geoid based vertical datum (NZVD2009). This provided New Zealand with the unified vertical datum, and better use of the GNSS technology within the country (Amos, 2010).

1.5 The AUSGeoid09 geoid model of Australia

The Australian gravimetric quasi geoid model of 2009 (AUSGeoid09) (Featherstone *et al*., 2011) was developed as an improvement from the AUSGeoid98 geoid model. The AUSGeoid09 quasi geoid model has been fitted to the Australian vertical datum to develop the AUSGeoid09 hybrid geoid model. The Australian Height Datum 1971 (AHD71) was

developed by setting the average value observed at 32 tide gauges around Australia between 1966 and 1968 to a height of 0.000 metres (Featherstone *et al*., 2011).

The availability of the new dataset from the Gravity Recovery and Climate Experiment (GRACE) and the EGM2008 geopotential model led to the computation of a new AUSGeoid gravimetric quasi geoid model of 2009 (AUSGeoid09). The AUSGeoid09 gravimetric quasi geoid model was developed to improve the quality of the AHD71 datum (Featherstone *et al*., 2010). It provides a better model of the surface of zero elevation of the AHD71 datum.

The long wavelength component of the AUSGeoid09 model was computed from the spherical harmonic coefficients of EGM2008 global gravimetric model, complete to degree and order 2190 (Featherstone *et al*., 2010).

The short wavelength component was computed from the residual mean gravity anomalies. The residual mean gravity anomalies are computed from subtracting the $1' \times 1'$ grid of EGM2008 gravity anomalies from the merged land ocean grid gravity anomalies. This contribution was computed using the 1D-FFT numerical integration technique for different kernel modification of the spherical Stokes' function (Featherstone *et al*., 2011).

The Molodensky term (G_1) (terrain effect) was computed from the $9'' \times 9''$ GEODATA-DEM9S Australian digital elevation model (Featherstone *et al*., 2011). The contribution of the terrain effect is used to transform the AUSGeoid09 gravimetric geoid model to AUSGeoid09 quasi geoid model. The AUSGeoid09 quasi geoid model was validated using 911 GPS/levelling data points (Featherstone *et al*., 2010).

The correction surface was computed using least squares collocation cross validation technique. The AUSGeoid09 hybrid geoid model was developed after fitting the correction surface on the AUSGeoid09 quasi geoid model. The correction surface removes the existing tilt and distortion on the AUSGeoid09 quasi geoid model (Featherstone *et al*., 2010).

The standard deviation of the AUSGeoid09 quasi geoid model has been reduced from ± 231mm to ± 30mm after fitting the correction surface. The AUSGeoid09 hybrid geoid model is a more preferable product for Australian GNSS heighting (Featherstone *et al*., 2010).

1.6 U.S.A (North America) geoid model based vertical datum

The National Geodetic Surveys (NGS) is a program required to define, maintain, and provide access to the National Spatial Reference System (NSRS). There are two existing vertical datums in NSRS, National American Datum of 1983 (NAD83) (Roman *et al*, 2009), and the National American Vertical Datum of 1988 (NAVD88). The NAD83 is used as the ellipsoidal datum which is suitable for GPS surveys while NAVD88 is the orthometric datum suitable for levelling surveys (Roman *et al*, 2009).

The recently released geoid models over the region of United States includes the United States Gravimetric Geoid of 2009 (USGG2009), and the hybrid geoid height model is GEOID09. The USGG2009 is computed from the EGM2008 geopotential model based on GRACE (Palvis *et al,* 2008) gravity satellite mission data (Roman *et al*, 2009).

The GEOID09 was computed to fit the control data where GPS-derived NAD83 ellipsoidal heights were known on levelled NAVD 88 bench marks (GPSBMs). The GPS-derived ellipsoidal heights on levelled Bench Marks available in 2009 are referred to as GPSBM2009 (Roman *et al*, 2009). The conversion surface was computed from the GPSBM2009 (Roman *et al*, 2009) control data. The conversion surface was used to convert USGG2009 into GEOID09 hybrid geoid model. The resulting geoid height model would convert between NAD83 and NAVD88.

The least squares collocation method was used to model the systematic effects in residuals formed at the GPSBMs (Roman *et al*, 2009). The GEOID09 hybrid geoid model fits the GPSBM2009 control points at 1.5cm RMSE (Roman *et al*, 2009) relative to the official U.S.A. datums (Roman *et al*, 2009).

The current gravimetric geoid model for U.S.A is known as USGG2012. The USGG2012 (Roman and Weston 2011) geoid model was converted to GEOID12 hybrid geoid model (Roman and Weston 2011) from the GPSBM2012 control points. They have been computed using similar techniques as previous models. The accuracy of GEOID12 to NAVD88 nationwide is characterised by a misfit of $\pm 1.7cm$ relatively (Roman and Weston 2012).

This model was defined as the best current representation of the geopotential surface (W_0) with the value of $62{,}636{,}856.00\ m^2/s^2$ (Roman and Weston 2012). This surface was selected as the best fit through tide gauges through Canada and the United States when the

effects of Sea Surface Topography (SST) were taken into account (Roman and Weston 2012). This provides the best estimate of mean sea level in all of North America (Roman and Weston 2012).

This value was adopted by many other countries as an estimate of global mean sea level. This surface was adopted by Canada and will be used to define their Canadian Gravimetric Geoid model of 2013 (CGG2013) (Roman and Weston 2012), which became their official vertical datum definition in the year 2013. The United States will also follow with a similar adoption of a gravimetric geoidal height model as the means for determining heights presumably about 2022 (Roman and Weston 2012).

1.7 Geoid model for South America

The South American Gravity studies (SAGS) project established the fundamental gravity network (FGN) in South America. This fundamental was initiated to densify gravity data in South America. There are few countries who participated on this gravity surveys in recent years such as Argentina, Bolivia, Brazil, Ecuador, Paraguay, and Venezuela (Blitzkow *et al*, 2016).

The data was used for computation of the gravimetric geoid model of 2015 (GEOID2015) (Blitzkow *et al*, 2016). The GEOID2015 geoid model is bounded within $15°N\ and\ 57°S\ latitude$ and $30°W\ and\ 97°W\ longitude$. The long wavelength component of the GEOID2015 geoid model was computed from the EIGEN-6C4 gravimetric model complete to degree and order 200 (Blitzkow *et al*, 2016).

The coastal areas were completed with mean free-air gravity anomalies derived from DTU10 model (Blitzkow *et al*, 2016). The Stokes' integral was evaluated using the fast Fourier transform (FFT) technique for computation of the short wavelength component.

The GEOID2015 geoid model has been evaluated against 1,319 GPS/levelling data points, 592 GPS/levelling data points are located in Brazil and the rest are distributed over the other countries. The GEOID2015 geoid model compared to the GPS/levelling data points over South America and Brazil with RMS of 46cm and 17cm respectively (Blitzkow *et al*, 2016).

1.8 **Research objective**

1. Computation of the gravimetric geoid model over the province of Gauteng. The long wavelength component of the geoid model is computed from the EGM2008 (Pavlis *et al*, 2009) geopotential model truncated at degree 720.
2. The available terrestrial gravity data set from the South African Council of Geoscience is used for computation of the short wavelength component, distributed only within the Gauteng province. It is identical to the data set used by Merry (2009) for computation of the SAGEOID2010 geoid model.
3. The evaluation of the Stokes' integral was undertaken using both fast Fourier transform and the least squares collocation techniques. The consistency of the results between the two techniques and their relative computational efficiency are compared.
4. The geoid models from the study are then compared to the SAGEOID2010 hybrid geoid model for evaluating any improvement in their accuracy.
5. The long wavelength component of the computed geoid model will be compared to the full EGM2008 geopotential model over selected number of data points in Gauteng province.

2 THE THEORY OF LOCAL GEOID MODELLING

2.1 Gravimetric geoid model components

It is currently a standard practice to compute the geoidal height at a point by evaluating the attributes in terms of the following component:

$$N = N_L + N_S + N_I, \quad (2:1)$$

Where:-

$N -$ Total geoidal height anomaly at the computation point,

N_L −Long wavelength component,

$N_S -$ Short wavelength component/ inner zone,

$N_I -$ Innermost zone component

The long wavelength component is computed using a geopotential model comprising of a global set of spherical harmonic coefficients as elaborated in section 2.2. There are a number of available geopotential models, such as, EGM2008 (Pavlis *et al*, 2008), EIGEN-CG03C (Fõrste *et al*, 2005), and many more.

The WGS84 ellipsoid was used as the reference ellipsoid for geoid modelling in this study. The parameters of the reference ellipsoid are as specified on the table:

Table 2-1: Parameters of the WGS84 reference ellipsoid.

Parameter	Notation	Value
Semi-major axis	a	6378137.0m
Flattening Factor of the Earth	$1/f$	298.257223563
angular velocity of the earth rotation	ω	7292115 x 10^{-11} radians/second
Gravity mass constant	GM	3986005 x 10^8 m^3/s^2

2.2 The long wavelength component of the geoid model

The computation of the long wavelength component from spherical harmonic coefficients of a geopotential gravimetric model will be described in detail. This will be very useful for computer programming. The long wavelength component is computed from the spherical harmonic coefficients of the EGM2008 geopotential model; this can be expressed as follow (Losch and Seufer, 2003):

$$N_L = \frac{GM_g}{\gamma_0(\bar{\varphi})r}.\sum_{n=2}^{n_{max}}\left(\frac{a_g}{r}\right)^n.\sum_{m=0}^{n}\left(\Delta\bar{C}_{n,m}\cos m\lambda + \bar{S}_{n,m}\sin m\lambda\right).\bar{P}_{n,m}(\sin\bar{\varphi}), \quad (2:2)$$

Where:-

$GM_g -$ Gravity mass constant of the geopotential model in m^3/s^2 defined from the geodetic model, $\gamma_0(\bar{\varphi}) -$ normal gravity in $m.s^{-2}$,

$r -$ Radial distance to the computational point also known as the local elliptic radius in metres m,

$a_g -$ Semi-major axis of the geopotential model,

$\bar{C}_{n,m}\ and\ \bar{S}_{n,m} -$ Fully normalised spherical harmonic coefficients (or Stokes' coefficients) of degree *n* and order *m*,

$\bar{P}_{n,m} -$ Fully normalised harmonics Legendre function,

$\bar{\varphi} -$ Geocentric latitude of the computation point,

$\varphi\ and\ \lambda -$ Geodetic latitude and longitude of the computation point

$\Delta\bar{C}_{n,m} -$ It is the difference between the full harmonic coefficient $\bar{C}_{n,m}$ and the harmonic coefficient generated by the normal gravity field $C^*_{n,m}$.

This difference is computed to correct the zonal coefficients of the spherical harmonic gravity model such as $\bar{C}_{2n,0}, where\ n = 1,2,3,4,5$ while the other $\bar{C}_{2n,0}$ are equal to zero (Losch and Seufer, 2003). The full harmonic coefficients ($S_{n,m}$) are non-zero (Merry, 2010).

$$\Delta\bar{C}_{n,m} = \bar{C}_{n,m} + \left(\frac{GM}{GM_g}\right)\left(\frac{a}{a_g}\right).C^*_{n,m}, \quad (2:3)$$

Where:-

$GM -$ Gravity mass constant of the reference ellipsoid,

$a -$ Semi-major axis of the reference ellipsoid

The ${C^*}_{n,m}$ can be expressed as follow:

$$ {C^*}_{n,m} = \frac{J_{2n}}{\sqrt{4n+1}}. \tag{2:4} $$

The scaling factor for the geopotential model is determined by the fraction of the gravity mass constant and the semi-major axis $\left(\frac{GM}{GM_g}\right).\left(\frac{a}{a_g}\right)$. It is done to account for the differences between the gravity mass constant and the semi major axis for the geopotential model and the ellipsoid. It is important to do so when differencing two potentials from each other (potential of the model and the potential of the ellipsoid) (Losch and Seufer, 2003).

The coefficient J_{2n} is computed from parameters a, *f*, and the angular velocity ω of the earth's rotation, this can be expressed as follow (Losch and Seufer, 2003:

$$ J_{2n} = (-1)^{n+1} \frac{3\left(\frac{E}{a}\right)^{2n}}{(2n+1)(2n+3)}\left(1 - n + 5n\frac{C-A}{ME^2}\right), \tag{2:5} $$

Where:-

$C -$ The moment of inertia with respect to the axis of rotation (not to be confused with the spherical harmonic coefficients $\overline{C}_{n,m}$),

$A -$ The moment of inertia with respect to any axis in the equatorial plane,

$M -$ Total mass,

$E -$ The linear eccentricity which can be expressed as follow:

$$ E = \sqrt{a^2 + b^2} \tag{2:6} $$

It is computed from the reference ellipsoid parameters. The final equations for the quantities mentioned can be expressed as follow (Losch and Seufer, 2003):

$$\left(\frac{C-A}{ME^2}\right) = \frac{1}{3}\left[1 - \frac{2}{15}\left(\frac{me'}{q_0}\right)\right], \tag{2:7}$$

$$m = \frac{\omega^2 a^2 b}{GM}, \tag{2:8}$$

$$q_0 = \frac{1}{2}\left[\left(1 + \frac{3}{e'^2}\right)\arctan e' - \frac{3}{e'}\right]. \tag{2:9}$$

Where:-

e' – Is the second numerical eccentricity, this can be expressed as follow (Losch and Seufer, 2003):

$$e' = E/b. \tag{2:10}$$

Much focus must be put in the computation of the J_{2n} coefficients since it is a very large value, which will be differenced with another large value. Any minor error may results in a larger error in the solution (Losch and Seufer, 2003).

2.2.1 Computation of the Legendre polynomial

The associated Legendre functions given by $P_{n,m}(\sin\bar{\varphi})$ and the fully normalised Legendre functions are given by $\overline{P}_{n,m}(\sin\bar{\varphi})$. The abbreviation $t = \sin\bar{\varphi}$ and $u = \cos\bar{\varphi}$ will be used for convenience. It is sometimes called the fully normalised harmonics. The first order of the Legendre's functions of the first kind is defined as (Heiskanen and Moritz, 1967):

$$P_{n,m}(t) = \frac{1}{2^n n!}(1-t^2)^{\frac{m}{2}}\frac{d^{n+m}}{dt^{n+m}}(t^2-1)^n, \tag{2:11}$$

The associated Legendre functions can be computed using recursive formulas such as (Losch and Seufer, 2003):

$$\begin{aligned} P_{n+1,0}(t) &= (2n+1)tP_{n,0}(t) - nP_{n-1,0}(t)\,, \\ P_{n,n}(t) &= (2n-1)\sin\theta\, P_{n-1,n-1}(t), \\ P_{n,m}(t) &= P_{n-2,m}(t) + (2n-1)\sin\theta\, P_{n-1,m-1}(t). \end{aligned} \tag{2:12}$$

With the beginning values as follow:

$$\begin{aligned} P_{0,0}(t) &= 1, \\ P_{1,0}(t) &= t, \;\; P_{1,1}(t) = u \end{aligned}$$

$$P_{2,0}(t) = \frac{3}{2}t^2 - \frac{1}{2},$$

$$P_{2,1}(t) = 3ut, \qquad P_{2,2}(t) = 3u^2.$$

The fully normalised associated Legendre functions are computed using a recursive method. There is a sectorial and non-sectorial type of recursive method. The following recursion formula for $\bar{P}_{n,m}(t)$using non sectorial $(i.e.\ n > m)$ method can be expressed as follow (Holmes and Featherstone, 2001):

$$\bar{P}_{n,m}(t) = a_{n,m}\, t\, \bar{P}_{n-1,m}(t) - b_{n,m}\bar{P}_{n-2,m}(t), \qquad for\ all\ n > m \tag{2:13}$$

Where:-

$$a_{n,m} = \sqrt{\frac{(2n-1)(2n+1)}{(n-m)(n+m)}}, \tag{2:14}$$

$$b_{n,m} = \sqrt{\frac{(2n+1)(n+m-1)(n-m-1)}{(n-m)(n+m)(2n-3)}}, \tag{2:15}$$

The recursion formula for $\bar{P}_{m,m}(t)$ using sectorial method $(i.e. n = m)$ is used to serve as seed values for the recursion in equation (2:13). This is computed using the initial values $\bar{P}_{0,0}(t) = 1\ and\ \bar{P}_{1,1}(t) = \sqrt{3}\,u$. The values for higher degree and order can be computed as follow (Holmes and Featherstone, 2001):

$$\bar{P}_{m,m}(t) = u\sqrt{\frac{2m+1}{2m}}\,\bar{P}_{m-1,m-1}(t), \qquad for\ all\ m > 1, \tag{2:16}$$

The figure (2-1) below demonstrates the behaviour of the complete recursion process in equation (2:13) and (2:16) using the lower triangular matrix. The circles on the figure (2-1) correspond to a particular combination of degree and order. Each circle represents a value of $\bar{P}_{n,m}(t)$, as well as the corresponding pair of recursive terms $a_{n,m}\ and\ b_{n,m}$ (Holmes and Featherstone, 2001).

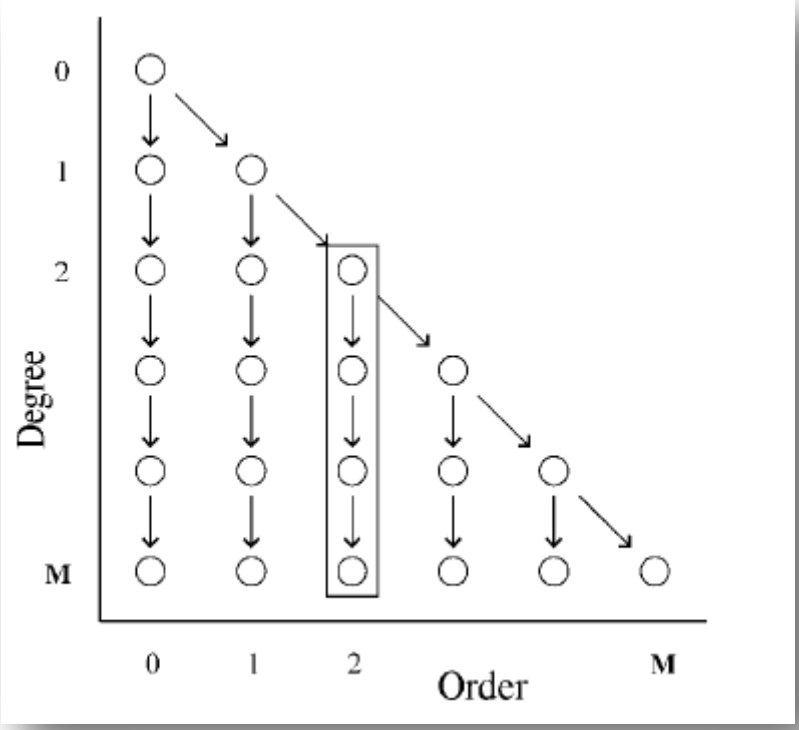

Figure 2-1: Schematic of the recursion sequences employed in the standard, first modified and second modified forward column algorithms to compute $\bar{P}_{n,m}(t)$ (Holmes and Featherstone, 2001).

It is highly recommended to use the recursion method for computation of the $\bar{P}_{n,m}(t)$, since it is numerically stable for higher degree and order, especially for computer programming. An explicit expression for the associated Legendre function can be expressed as follow (Moritz, 1980):

$$P_{n,m}(t) = 2^{-n}(1-t^2)^{\frac{m}{2}} \sum_{k=0}^{r} (-1)^k \frac{(2n-2k)!}{k!\,(n-k)!\,(n-m-2k)!} t^{n-m-2k}, \quad (2:17)$$

The term r is the greatest integer from $\leq (n-m)/2$; whichever is an integer between $(n-m)/2$ or $(n-m-1)/2$. The Legendre functions are defined by polynomial functions of $\sin\bar{\varphi}$ (Moritz, 1980).

Then the associated Legendre function is fully normalised using the following (Losch and Seufer, 2003):

$$\bar{P}_{n,m}(t) = \sqrt{k(2n+1))\frac{(n-m)!}{(n+m)!}}P_{n,m}(t), \quad (2:18)$$

$$with\ k = \begin{cases} 1\ for\ m = 0 \\ 2\ for\ m \neq 0 \end{cases}$$

The higher the degree and order, this method gets to be numerically unstable. That may be caused by the factorial of a larger number.

The spherical harmonics models are formulated from the centre of the earth so geocentric geodetic coordinates are used in the computation of the geoid undulation. The longitude remains the same for both geocentric and geographic coordinates. The latitude used has to be converted from geographic φ to geocentric latitude $\bar{\varphi}$. This can be computed as follow (Losch and Seufer, 2003):

$$\bar{\varphi} = arctan\frac{z}{\sqrt{x^2 - y^2}} = \arctan\left[\left(\frac{b}{a}\right)^2 \tan\varphi\right]. \quad (2:19)$$

The normal gravity is the function of latitude is as given below (Heiskanen and Moritz, 1967):

$$\gamma_0(\bar{\varphi}) = \gamma_a\frac{1 + \kappa sin^2\bar{\varphi}}{\sqrt{1 - e^2 sin^2\bar{\varphi}}}, \text{with } \kappa = \frac{b\gamma_b - a\gamma_a}{a\gamma_a} \quad (2:20)$$

Where:-

$a -$ Semi-major axis of the reference ellipsoid,

$b -$ Semi-minor axis of the reference ellipsoid,

$\gamma_a and\ \gamma_b -$ The normal gravity at the equator and at the pole,

$e -$ The first numerical eccentricity of the reference ellipsoid

The local elliptic radius $r(\bar{\varphi})$ is computed as follow (Losch and Seufer, 2003):

$$r(\bar{\varphi}) = \sqrt{x^2 + y^2 + z^2} = a\sqrt{1 + \frac{e^2(1 - e^2)sin^2\bar{\varphi}}{1 - e^2 sin^2\bar{\varphi}}}, \quad (2:21)$$

It can also be approximated as:

$$r(\bar{\varphi}) = a(1 - f sin^2\bar{\varphi}). \quad (2:22)$$

Where:-

f − Flattening parameter from the reference ellipsoid

Then all the quantities can be put together to compute the long wavelength component as a function of spherical harmonic coefficients of a gravimetric geoid, this is as expressed by equation (2:2) above.

2.3 Computation of the short wavelength component

The traditional numerical integration method was used to evaluate Stokes' integral. Currently, there are two techniques used for evaluation of the Stokes' integral, known as, least squares collocation and fast Fourier transform. It is the most important formula in physical geodesy since it allows the determination of the geoid from gravity data.

The Stokes' formula or Stokes' integral was published in 1849 by George Gabriel Stokes. The Stokes' integral for computation of the short wavelength component is expressed as follow (Heiskanen and Moritz, 1967):

$$N = \frac{R}{4\pi\gamma} \iint_{\sigma} \Delta g . S(\psi) d\sigma \tag{2:23}$$

Where:-

R − Mean radius of the Earth,

Δg − Gravity anomalies,

ψ − Geocentric angle/ spherical distance,

$d\sigma$ − Is an infinitesimal surface element of the unit sphere σ,

$S(\psi)$ − Stokes' function,

The Stokes' Kernel function can be computed as follow (Heiskanen and Moritz, 1967):

$$S(\psi) = \frac{1}{\sin(\frac{\psi}{2})} - 6\sin\frac{\psi}{2} + 1 - 5\cos\psi - 3\cos\psi \,.\ln\left[\sin\frac{\psi}{2} + \sin^2\frac{\psi}{2}\right]. \tag{2:24}$$

This can be expressed in elements of $\sin\frac{\psi}{2}$ as follow:

$$S(\psi) = \frac{1}{\sin\frac{\psi}{2}} - 4 - 6\sin\frac{\psi}{2} + 10sin^2\frac{\psi}{2} - \left[3 - 6sin^2\frac{\psi}{2}\right]\ln\left[\sin\frac{\psi}{2} + \sin^2\frac{\psi}{2}\right], \quad (2:25)$$

Where $\sin^2\frac{\psi}{2}$ can be reduced as follow:

$$\sin^2\frac{\psi}{2} = \sin^2\frac{\delta\varphi}{2} + \sin^2\frac{\delta\lambda}{2}\cos\varphi_P\cos\varphi, \quad (2:26)$$

$$\delta\varphi = \varphi_P - \varphi, \qquad \delta\lambda = \lambda_P - \lambda. \quad (2:27)$$

Where:-

(φ_P, λ_P) − Geographical coordinates of the centre of the grid or block,

(φ, λ) − Geographical coordinates of the computational point,

$\bar{\varphi}$ − Geocentric latitude of the computation point

In a case were $\varphi = \varphi' \; and \; \lambda = \lambda'$ then $\psi = 0$ (Sideris & She, 1994).

2.4 Evaluation of the Stokes' integral using least squares collocation

The basic principle of least squares adjustment is to determine a model to minimise the sum of the squares of the residuals (corrections) for the observed quantities. A system of linear equations of order equal to the number of observed quantities is generated for the least squares adjustments.

The least squares collocation (LSC) theory is used in physical geodesy for the solution of the gravimetric boundary value problem. The Wiener-Hopf approach uses least squares prediction for the interpolation of the gravity anomalies on the terrestrial sphere (of radius R) (Moritz, 1978).

It is a classical technique used in various applications of geodesy and photogrammetry. The parametric case of least squares adjustment can be expressed as follow (Moritz, 1972):

$$x = AX + n \quad (2:28)$$

Where:-

x − Observation vector (n x 1),

$A -$ Represent a design matrix or Jacobian matrix containing the coefficients of the unknown parameters, with a size of (n x u),

$X -$ Represent a solution vector or a vector of unknown parameters, with a size of (u x 1),

$n -$ Represent a residuals or noise vector, with a size of (n x 1).

The values for n and u above represent the total number observations and the total number of unknown parameters. Collocation is defined as the determination of a function by fitting an analytical approximation to a certain number of given linear functions (Moritz, 1980). The generalised least squares collocation model can be expressed as follow (Moritz, 1972):

$$x = AX + s + n \tag{2:29}$$

In addition to the noise quantity, a signal quantity is added as the second random quantity. All the other quantities are the same as in equation (2:28) above. The signal value can be estimated or predicted at the computation point using the least squares collocation (LSC) technique. The least squares interpolation uses the Wiener-Kolmogorov prediction formula from the theory of stochastic processes; this can be expressed as follow (Moritz, 1972):

$$s_P = [C_{P1}\ C_{P2}\ \dots\ C_{Pn}]\begin{bmatrix} \bar{C}_{11} & \bar{C}_{12} & \cdots & \bar{C}_{1n} \\ \bar{C}_{21} & \bar{C}_{22} & \cdots & \bar{C}_{2n} \\ \vdots & \vdots & \ddots & \vdots \\ \bar{C}_{n1} & \bar{C}_{n2} & \cdots & \bar{C}_{nn} \end{bmatrix}^{-1}\begin{bmatrix} l_1 \\ l_2 \\ \vdots \\ l_n \end{bmatrix} \tag{2:30}$$

This can be abbreviated as follow:

$$s_P = C_{pi}\bar{C}_{ij}{}^{-1} l_i. \tag{2:31}$$

Where:-

$$l = s + n = x - AX$$

$AX -$ Observations systematic effects

$C_{Pi} -$ Signal covariance function vector,

$\bar{C}_{ij} -$ Cross covariance matrix, between the interpolated value and the observed.

The following is the list of some applications of the least squares collocation defined by Moritz (1972):

i. Gravity measurements: Gravimeter reading is the observation, signal is the gravity anomaly and noise occurs due to random measuring error. The vector X includes parameters of two kinds, normal gravity formula parameters and instrumental constants.
ii. Satellite observations: The x vector comprises of optical or electronic measurements to artificial satellites, linearization of normal orbit gives AX. Gravitational perturbations are the signal and noise comprises of measuring errors and other random effects.
iii. Transformations in remote sensing: In geodetic coordinate transformations residual distortions may remain behind which are strongly correlated. AX is the transform formula, residual distortions give the signal and noise is due to measuring errors.

The least squares collocation method requires the choice of a reproducing kernel which is a local covariance function.

2.4.1 Interpolation of the gravity anomalies by LSC

The gravity anomalies can be computed from the disturbing potential using the relationship expressed using equation (a) in **Appendix A**. The gravity anomaly on the sphere can be interpolated from the gravity anomaly measured on the surface of the earth using least squares interpolation technique. This can be expressed as follow (Moritz, 1978).

$$\Delta g_p^* = C_{pi}\bar{C}_{ij}^{\ -1}\Delta g_i \tag{2:32}$$

Where:-

Δg_i – Measured gravity anomalies on the surface of the earth at the fixed point,

C_{pi} – Covariance function vector of the gravity anomalies,

$\bar{C}_{ij}$ – Error covariance matrix, an identity matrix is used in this case since no further details were given for the observed gravity anomalies

In this case the systematic effects are assumed to be zero (i.e. $AX = 0$). The covariance function of the disturbing potential to the data points outside the sphere can be expressed as follow (Moritz, 1972):

$$K(P \quad \sum \left(\text{—}\right)^{(n} \quad \bar{P}\ (\cos \tag{2:33}$$

Where:-

$\bar{P}_n(\cos \quad) -$ Fully normalised Legendre's polynomial functions,

– Spherical distance between two points on a sphere,

Local ellipsoidal radius of point , respectively

– Coefficient computed from the harmonic coefficients as follow:

$$\sum (\bar{a} \quad - \quad) \tag{2:34}$$

Where:-

$\bar{a} \quad \bar{b}_{nm}$ – are the coefficients of fully normalised harmonics.

The spherical distance is computed using the following expression (Hofmann-Wellenhof and Moritz, 2005):

$$[\cos \quad \cos(\lambda \quad)], \tag{2:35}$$

The disturbing potential is harmonic outside the sphere to satisfy Laplace's as expressed by equation (b) in **Appendix A**. The corresponding covariance function of the gravity anomaly can be expressed as follow (Moritz, 1970):

$$(P \quad (\Delta \tag{2:36}$$

Then:-

$$C(P \quad \sum \left(\text{—}\right)^{(n} \quad \bar{P}\ (\cos \tag{2:37}$$

Where:-

– Coefficient computed from the harmonic coefficients as follow:

$$c_n = \left(\frac{n-1}{R}\right)^2 k_n \tag{2:38}$$

The measured gravity anomalies are assumed to be errorless in this case. The covariance functions $K(P,Q)$ and $C(P,Q)$ can be related to each other by c_n and k_n, this shows that one function can be computed from the other (Moritz, 1972).

The interpolated gravity anomalies can be expressed as follow in matrix form using least squares interpolation:-

$$\Delta g_p^* = \begin{bmatrix} C_{p1} & C_{p2} & \dots & C_{pn} \end{bmatrix} \begin{bmatrix} \bar{C}_{11} & \bar{C}_{12} & \cdots & \bar{C}_{1n} \\ \bar{C}_{21} & \bar{C}_{22} & \cdots & \bar{C}_{2n} \\ \vdots & \vdots & \ddots & \vdots \\ \bar{C}_{n1} & \bar{C}_{n2} & \cdots & \bar{C}_{nn} \end{bmatrix}^{-1} \begin{bmatrix} \Delta g_1 \\ \Delta g_2 \\ \vdots \\ \Delta g_n \end{bmatrix} \tag{2:39}$$

The condition of the least squares adjustment is to determine a model to minimise the sum of the squares of the residuals (corrections) for the observed quantities. The residuals of the measured data points are expressed as follow as:

$$V = \Delta g_P - \Delta g_P^* \tag{2:40}$$

Where:-

$\Delta g_P -$ Observed mean gravity anomaly of a grid,

$\Delta g_P^* -$ Interpolated mean gravity anomaly of a grid

With variance:-

$$\sigma^2 = V^T P V / n \tag{2:41}$$

$$\sigma^2 = (\Delta g_P - \Delta g_P^*)^T P (\Delta g_P - \Delta g_P^*)/n \tag{2:42}$$

The weight matrix is denoted by P. In this case an identity matrix has been used for the weight matrix since no accuracy details have been provided for the observed gravity anomalies.

The interpolated gravity anomalies will now be used for computing the geoidal height, using the Stokes' integral. Least squares collocation will be used for evaluation of the Stokes' integral in the follow subsection.

2.4.2 Geoid undulation using least squares collocation

The evaluation of the Stokes's integral provides correction to the geoidal heights computed from the spherical harmonic coefficients. It reduces observation errors provided by the gravity data. The large proportion of this error can be reduced using the high-degree global geopotential model (Featherstone & Vella, 1999).

All these quantities, such as gravity anomalies, geoidal height, deflection of the vertical and many more, can be derived from the differential potential T. Using linear operations such as differentiation or integral formulas. In the same way all signal covariance functions may be derived from one basic covariance function, the covariance function of the differential potential by the corresponding linear operation (Moritz, 1972).

The geoidal height computed from the gravity anomalies by Stokes's integral as expressed by equation (2:23) above. It can be abbreviated in matrix form as (Moritz, 1972):

$$N_P = L_{PA}\Delta g_A \tag{2:43}$$

Where:-

L_{PA} – Is the linear operator acting on Δg_A to transform it into geoidal height (N_P), in this case L_{PA} denotes the application of the Stokes' integral.

The covariance between the gravity anomalies at a point P and geoidal height at a point Q can be computed using the law of propagation of co-variances (Moritz, 1972). This can be abbreviated as follow:

$$cov(\Delta g_P, N_Q) \tag{2:44}$$

Each quantity can be determined as follow (Moritz, 1972):

$$\Delta g_P = -\left(\frac{\partial T}{\partial r}\right)_P - \frac{2}{R}T_p, \tag{2:45}$$

$$N_Q = \frac{1}{\gamma}T_Q, \tag{2:46}$$

The operator that determines the geoidal height from T is applied to the covariance function of the T (i.e. $K(P,Q)$), this can be expressed as follow (Moritz, 1972):

$$N_Q = \frac{1}{\gamma}K(P,Q), \tag{2:47}$$

Then applying the operation that determines Δg from T, this can be expressed as follow (Moritz, 1972):

$$\Delta g_P = -\frac{\partial}{\partial r_P}\left(\frac{1}{\gamma}K(P,Q)\right) - \frac{2}{R}\left(\frac{1}{\gamma}K(P,Q)\right), \tag{2:48}$$

Therefore, the covariance function between the gravity anomalies and the geoidal height can be expressed as follow (Moritz, 1972):

$$cov(\Delta g_P, N_Q) = -\frac{1}{\gamma}\frac{\partial K(P,Q)}{\partial r_P} - \frac{2}{\gamma R}K(P,Q), \tag{2:49}$$

Furthermore, after the derivative of the disturbing potential covariance function with respect to r_P, the above equation (2:49) can be expressed as follow:

$$cov(\Delta g_P, N_Q) = -\frac{1}{\gamma}G_n - \frac{2}{\gamma R}K(P,Q), \tag{2:50}$$

Where:-

$$G_n = \frac{\partial K(P,Q)}{\partial r_P} = -\sum_{n=2}^{n_{max}} k_n.(n+1)\left(\frac{R^2}{r_P r_Q}\right)^n.\left(\frac{R^2}{{r_P}^2 r_Q}\right)\bar{P}_n(\cos\psi_{PQ}), \tag{2:51}$$

This give evidence that the geoidal height can be computed using lease squares collocation technique. The covariance function between the gravity anomalies and the geoidal height is used for vector C_{pi}. The cross covariance matrix ($\bar{C}_{ij}$) is determined by the residual between the interpolated gravity anomalies and the observed gravity anomalies. Therefore, the geoidal height can be computed from the least squares collocation using equation (2:31) above as follow:

$$N_P = C_{pi}{\bar{C}_{ij}}^{-1}\Delta g_P^*. \tag{2:52}$$

Below are the properties of least squares collocation defined by Moritz (1972):

i. Both measured and computed quantities maybe quite heterogeneous.
ii. The observations may be errorless or affected by measuring errors (noise).
iii. The method is invariant with respect to linear transformations of the data or of the results.
iv. The solution is optimal in the sense that it gives the most accurate results obtainable on the basis of the available data.

2.5 Evaluation of the Stokes' integral using fast Fourier transform

The Stokes' integral expressed by equation (2:23) above can be evaluated by the 1D-FFT method as follow (Featherstone & Vella, 1999):-

$$N(\varphi_i, \lambda_i) = \frac{R\Delta\varphi\Delta\lambda}{4\pi\gamma} \sum F^{-1}\left[\sum F\{\overline{\Delta g}(\varphi_P, \lambda_P)\cos\varphi_p\} F\{S(\psi_{Pi})\}\right] \quad (2:53)$$

Where:-

$F -$ Represent the direct one dimensional Fourier transform operator,

$F^{-1} -$ Represent the inverse Fourier transform operator

$\varphi_p, \lambda_P -$ Latitude and longitude at the centre of the grid

$\Delta g(\varphi_P, \lambda_P) -$ Residual gravity anomaly at the centre of the grid

The FFT technique is considered as the spectral solution to the classical boundary value problem. The spectral functions for the gravity anomalies $\Delta G(u, v)$, and the Stokes function $S(u, v)$ can be expressed as follow (Sideris et al, 1989):

$$\Delta G(u, v) = \int_{-\infty}^{\infty}\int_{-\infty}^{\infty} \overline{\Delta g}(\varphi_P, \lambda_P).e^{-2\pi i(u\varphi_P + v\lambda_P)}.\cos\varphi_p\, d\varphi d\lambda = F\{\overline{\Delta g}(\varphi_P, \lambda_P)\cos\varphi_p\} \quad (2:54)$$

$$S(u, v) = \int_{-\infty}^{\infty}\int_{-\infty}^{\infty} S(\Delta\varphi, \Delta\lambda).e^{-2\pi i(u\Delta\varphi + v\Delta\lambda)}\, d\varphi d\lambda = F\{S(\Delta\varphi, \Delta\lambda)\} \quad (2:55)$$

The (u, v) are the wavenumbers corresponding to the (φ, λ) spatial coordinates respectively and i is the imaginary unit ($i = \sqrt{-1}$). Therefore, the geoid undulation is computed from the inverse of the product of the two spectral functions (2:54) and (2:55) (Sideris et al, 1989). Stokes' function can be expressed as a function of spherical distance as give in series form below (Featherstone & Vella, 1999):

$$S(\psi_{Pi}) = \sum_{n=2}^{n_{max}} \left(\frac{2n+1}{n-1}\right) P_n(\cos\psi_{Pi}) \quad (2:56)$$

The spherical distance (ψ_{Pi}) is computed between the data point (φ_i, λ_i) and the centre of the grid (φ_P, λ_P). The size of the grid for the data is $(X \times Y)$ and it is divided into blocks of $(\Delta\varphi \times \Delta\lambda)$ around the computational points. This can be depicted in the figure (2-2) below:

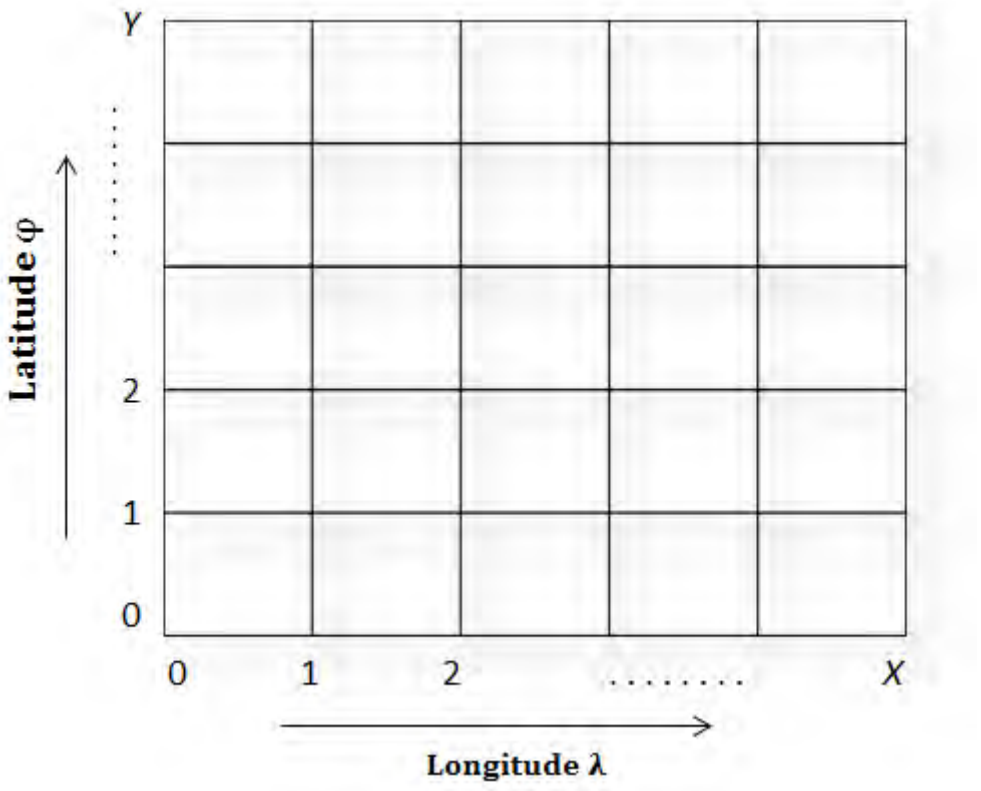

Figure 2-2: Schematic diagram of (X x Y) grid divided into compartments.

Grid line which is the subdivision of the area of interest by means of grid lines of some fixed coordinates system, in particular of ellipsoidal coordinates φ, λ. The grid lines are plotted to form a rectangular or square blocks on a plane geometry, for example $10' \text{ X } 10' or\ 1^o \text{ X } 1^o$ (Hofmann-Wellenhof and Moritz, 2005). The figure (2-2) above depicts how the grid line method is used for the subdivision of the earth surface. The grid line method is mostly used for computer programming (Hofmann-Wellenhof and Moritz, 2005).

The advantage of the fixed blocks formed by gridlines determined by the ellipsoidal coordinates, it makes it easy for their data to be stored and process by a computer. Also in the gridline method only one subdivision can be used for all computation points (Hofmann-Wellenhof and Moritz, 2005).

There is an increase on both quality and quantity of data used for geoid determination. The data processing problems requires greater ability and has created a demand for efficient numerical solutions. The fast spectral technique uses data in gridded form (Schwarz et al, 1989).

The fast Fourier transform (FFT) technique can be used to evaluate the spherical Stokes formula. The one dimensional fast Fourier transform (or 1D-FFT) has been used in this study. It is considered to be the best technique for evaluation of the Stokes' function (Featherstone & Vella, 1999).

The 1D-FFT approach gives exactly the same results as the direct numerical integration. It only deals with one-dimensional complex array each time, resulting in a considerable saving in computer memory as compared to the 2D-FFT approach (Sideris, 2013). The 2D-FFT method produces approximated results of the numerical integration (Yun, 1999).

2.6 **The innermost zone**

At the point where (φ_P, λ_P) and (φ_i, λ_i) coincide, this will be dealt with as the singularity problem at $\psi = 0$, such block will be excluded by defining $S(\psi) = 0$ if $\psi = 0$. The influence of this central block to the geoidal height will be computed separately (Stranger van Hees, 1990), as follow:

$$N = \frac{r}{\gamma} . \Delta g \tag{2:57}$$

This is applicable if the central area would be a circle with radius r.

2.7 **Vertical Datum**

There are a number of horizontal surfaces and there are methods used for identifying the desired horizontal surfaces as the datum. The first one is defining a constant value of Earth's gravity potential, $W = W_0 = Const.$ (abstract option) and the second one whereby the chosen horizontal surface gives a specific approximation of the mean-sea level surface (Vaníček, 1991).

The concept of the geoid based vertical datum is that the geoid does not exist in nature, it is only approximated. There are two methods used for the approximation of the geoid model namely the direct solution and the indirect solution (Vaníček, 1991). The point of zero height (Point on the datum) is determined from the observations of the sea level variation measured using tide gauges, when using the direct solution, and while on the indirect solution the point of zero height (Point on the datum) is determined by computing the orthometric height on the terrain of the earth (Vaníček, 1991).

The spacing between the geoid model and the mean sea level is called the Sea Surface Topography (SST). The SST is caused by the sea dynamics and by prevailing meteorological phenomena, which is approximately 2m or less in magnitude (Vaníček, 1991).

The SST is determined from the three different techniques namely:-

i. Oceanic levelling,
ii. Satellite altimetry combined with geoidal heights, and
iii. Local –Zero frequency response analysis" for meteorological and other effects.

The combination of these techniques does not promise to improve the potential accuracy to be substantial. However for SST differences, slightly better accuracy can be acquired (Vaníček, 1991).

2.8 **Various geoid model applications**

The list below describes various applications of the geoid model by Ulotu (2009):

i. Vertical datum for orthometric heights.
ii. Determination of orthometric heights from ellipsoidal heights. Global Navigation Satellite Systems (GNSS) provide us with heights referring to geocentric ellipsoids; the ellipsoidal height is of little use for day-to-day requirements of height. Usually our need for height is in the form of orthometric or normal height, and to obtain these, geoid height is needed.
iii. Understanding of ocean circulation patterns and dynamics
iv. Description of the positions of satellites and ground stations in suitable reference frames. The fact that the geoid reflects gravity field irregularities means that, a better understanding of the geoid enables refinement of satellite orbits.
v. Oceanography, hydrographic surveying and maritime. The geoid is valuable for oceanographers, hydrographic surveyors and maritime industries in general as vessels navigate vast bodies of water. The knowledge of the geoid is essential to better model ocean currents and undersea mapping especially in soundings. Sea-going vessels can take advantage of the currents and characteristics of the ocean to plan faster and safer routes, which in turn will use less fuel (conservation) and cost less.

vi. Knowledge of the geoid is important to model geodynamical phenomena (e.g. polar motion, Earth rotation, crustal deformation). Geoid is useful in interpretation of precursors to geo-hazards research such as the study of post-glacial rebound, earthquakes, volcanoes, landslides, tsunamis, and mitigation.

vii. Vertical and horizontal control networks definition, establishment, transformation and adjustment.

viii. Vertical datum can easily be unified even when there's no access to certain region and when there are datum inconsistencies.

There are other existing applications in engineering and geosciences.

3 COMPUTATIONAL STANDARDS/METHODOLOGY

The following elaborate the approach used for the computation of the gravimetric geoid model.

3.1 The remove compute restore approach

The computation of the gravimetric geoid model uses the routine approach known as the remove-compute-restore technique. The long wavelength component of the geoid model is provided by the spherical harmonic coefficients of the global geopotential model; in this study an EGM2008 model is used. The short wavelength component is computed from the evaluation of the Stokes's integral (Sideris, 2013). The remove-compute-restore technique involves the removal of the gravity anomalies generated by the global geopotential model from the terrestrial gravity anomalies (Featherstone & Vella, 1999), this can be expressed as follow:

$$\Delta g_r = \Delta g_t - \Delta g_{GM}, \tag{3:1}$$

Where:-

$\Delta g_r -$ The reduced/residual gravity anomalies,

$\Delta g_t -$ Terrestrial gravity anomalies,

$\Delta g_{GM} -$ Gravity anomalies generated by the spherical harmonic coefficients,

The gravity anomalies generated by the spherical harmonic coefficients is evaluated by the following expression (Losch and Seufer, 2003):

$$\Delta g_{GM} = \frac{GM_g}{a_g.r}.\sum_{n=2}^{n_{max}}(n-1)\left(\frac{a_g}{r}\right)^n.\sum_{m=0}^{n}\left(\Delta\bar{C}_{n,m}\cos m\lambda + \bar{S}_{n,m}\sin m\lambda\right).\bar{P}_{n,m}(\sin\bar{\varphi}), \tag{3:2}$$

Where:-

$GM_g -$ Gravity mass constant of the geopotential model in m^3/s^3 defined from the geodetic model,

$r -$ Radial distance to the computational point also known as the local elliptic radius in metres m,

$a_g -$ Semi-major axis of the geopotential model,

$\bar{C}_{n,m}\ and\ \bar{S}_{n,m} -$ Fully normalised spherical harmonic coefficients (or Stokes' coefficients) of degree *n* and order *m*,

$\bar{P}_{n,m} -$ Fully normalised harmonics Legendre function,

$\bar{\varphi} -$ Geocentric latitude of the computation point,

$\varphi\ and\ \lambda -$ Geodetic latitude and longitude of the computation point.

The geoidal height is related to the gravity anomalies using Stokes's integral, it can be expressed using geographical coordinates as follow (Featherstone & Vella, 1999):

$$N_S(\varphi,\lambda) = \frac{R}{4\pi\gamma}\int_{\lambda_i=0}^{2\pi}\int_{\varphi_i=\frac{-\pi}{2}}^{\frac{\pi}{2}} \Delta g_{FA}\,.\,S(\psi)\cos\varphi\, d\varphi \mathrm{d}\lambda \tag{3:3}$$

Where:-

$R -$ Mean Earth radius given in metres (m),

$\gamma -$ Normal gravity in metres per second squared ($m.s^{-2)}$,

$S(\psi) -$ Represent the Stokes's function.

The residual gravity anomalies can be used in an adjusted form of Stokes's integral as follow (Featherstone & Vella, 1999):

$$N(\varphi_i,\lambda_i) = N_L(\varphi_i,\lambda_i) + \frac{R}{4\pi\gamma}\int_{\lambda_i=0}^{2\pi}\int_{\varphi_i=\frac{-\pi}{2}}^{\frac{\pi}{2}} \Delta g_r\,.\,S(\psi)\cos\varphi\, d\varphi \mathrm{d}\lambda \tag{3:4}$$

Where:-

$N_L(\varphi_i,\lambda_i) -$ Represent the long wavelength component of the geoid model. The geoidal heights generated by the corresponding degree (n_{max}) of the same global geopotential model are then restored to the solution as expressed by equation (3:4) above (Featherstone & Vella, 1999).

3.2 **Computer software**

Three computer programs were designed for this research using *python 2.7.3* language, they are as listed below:

i. *Geoidcal.py*:- This program performs the computation of the long wavelength component of the geoid model. Using equation (2:2), the long wavelength component was computed using spherical harmonic coefficients from the EGM2008 gravimetric model complete to an order and degree 720. The program was then used to compute a geoid model from gravity data distributed over the province of Gauteng, bound within $-28°0'0"$ $-24\ 0\ 0$ and $26\ 0\ 0" \leq \lambda \leq 30°0'0"$.

ii. *Geoidlsc.py*:- This program performs the computation of the short wavelength component using gravity anomalies on Stokes' integral. The Stokes' integral was evaluated using least square collocation technique as elaborated in section 2.4 above. The evaluation of the Stokes's integral provides correction to the geoidal heights computed from the spherical harmonic coefficients. It reduces observation errors provided by the gravity data.

iii. *Geoidfft.py*:- This program also performs the computation of the short wavelength component by using the 1D-FFT technique to evaluate the Stokes' integral as elaborated in section 2.5 above. A $0.3^o \times 0.3^o$ grid was used for computation of the local geoid model over the study area.

The geoid model computed using the least squares collocation method was named SiPLSC geoid model, and the geoid model computed using the 1D-FFT method was name SiPFFT geoid model.

Most of the plots for the purpose of data analysis were done using the software namely *Golden Software surfer 9.* Data contour plots are produced from the *Golden Software surfer 9* and the statistical results is produced for the loaded data.

The *Intgrid* software is used to interpolate the geoidal heights from a file containing data which is on regular grid, using the method of bilinear interpolation. The grid files consist of latitude, longitude and geoidal height values in regular grid and the input file consist of latitude and longitude values. The values in the data file are space delimited; the results in the output file are in the order of latitude, longitude and the interpolated geoidal height value.

4 DATA COMPILATION

The geoid model gives a best approximation of the figure of the earth. There are various type of data used for determining geoid model. The accuracy of the geoid model depends on the quality of the data used, its distribution, density of the data and the source. The data used in this study are described as follows:

4.1 The Earth Gravity Model for 2008 (EGM2008) global model

The EGM2008 global geoid model has been developed by the United State National Geo-Spatial Agency (NGA); it is also named as EGM08. It is determined from the combination solution based on 57 months of GRACE satellite to satellite data tracking and at a global grid set of 5'X5' of the terrestrial gravity anomalies (Pavlis *et al*, 2008). The EGM2008 is complete to degree and order 2159, and it can be extended to degree 2190 and order 2159 when converted to spherical harmonic coefficients (Pavlis *et al*, 2008).

The spatial resolution for EGM2008 is 9.3km x 9.3km on the equator which makes it to be six times higher than that of the EGM96. The accuracy of the EGM2008 can be improved to be 3-6 times higher than that of the EGM96 that depends on the area of interest and the mathematical function used either for determining the geoid undulation, and the vertical deflection (Pavlis *et al*, 2008). The figure 4-1 below depicts the EGM2008 global model:

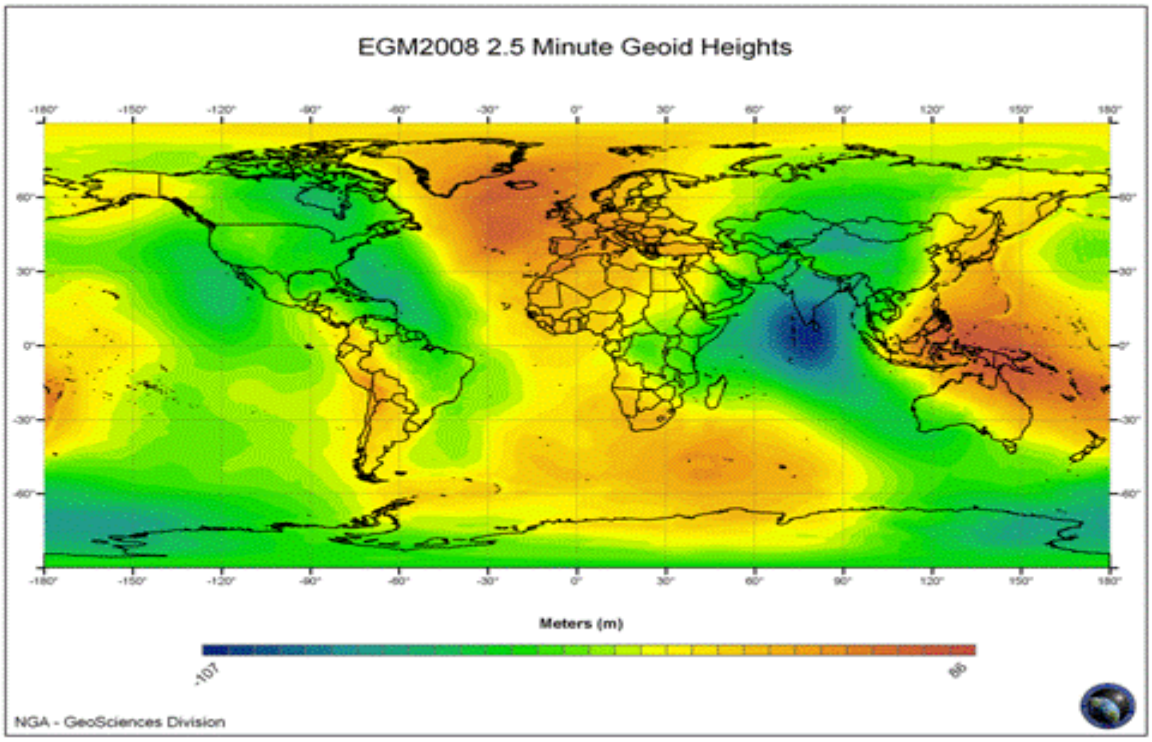

Figure 4-1: The Earth Gravimetric Model 2008 (Pavlis, 2008)

The satellite that was used is ITG-GRACE03 along with its complete error covariance matrix, the least squares adjustments was done to combine the only information from the GRACE satellite with the coefficients implied by terrestrial data. The EGM2008 does not contain any GPS/levelling or astronomic deflections of the vertical data (Pavlis *et al*, 2008).

Various types of coefficients were used into the spherical harmonic synthesis software for the computation of the geoid undulation. The EGM2008 geoid model has been provided into two types of grids for interpolation of the geoid undulations namely $1'X\,1'$ and the $2.5'X\,2.5'$ resolutions (Pavlis, 2008).

There are few GRACE based models beside EGM2008 such as GGM02C and EIGEN-GL04C which have the same performance in orbit computation and they all perform better than EGM96. The EGM2008 out performs all other models for terrestrial applications such as the Geoid undulations, deflection of the vertical and the dynamic ocean topography (Pavlis *et al*, 2008).

4.2 **The land gravity data**

The land gravity data provided was extracted from the primary gravity form the South African Council for Geoscience (formerly Geological Survey). Some 94952 values at an average spacing of less than 4km were provided (Merry, 2009). Additional data within South Africa and in neighbouring countries, within the data area bounded by $-39 < \phi < -18 \; and \; 12 < \lambda < 37$ were provided by several organisations.

In all, a total of 146740 values were available. These data were screened to check for duplicates. Where the separation was less than 2" (about 60m) the points were assumed to be duplicates and the most recent value used. The total number of duplicates was 1985. The discrepancies in gravity values at these points exceeded 2mgal in eight cases. Rather than use an erroneous value, all eight pairs of duplicates were removed from the data set. After removal of duplicates the total number of points available was 144747 (Merry, 2009). The following figure 4-2 depicts the data set distribution over South Africa:

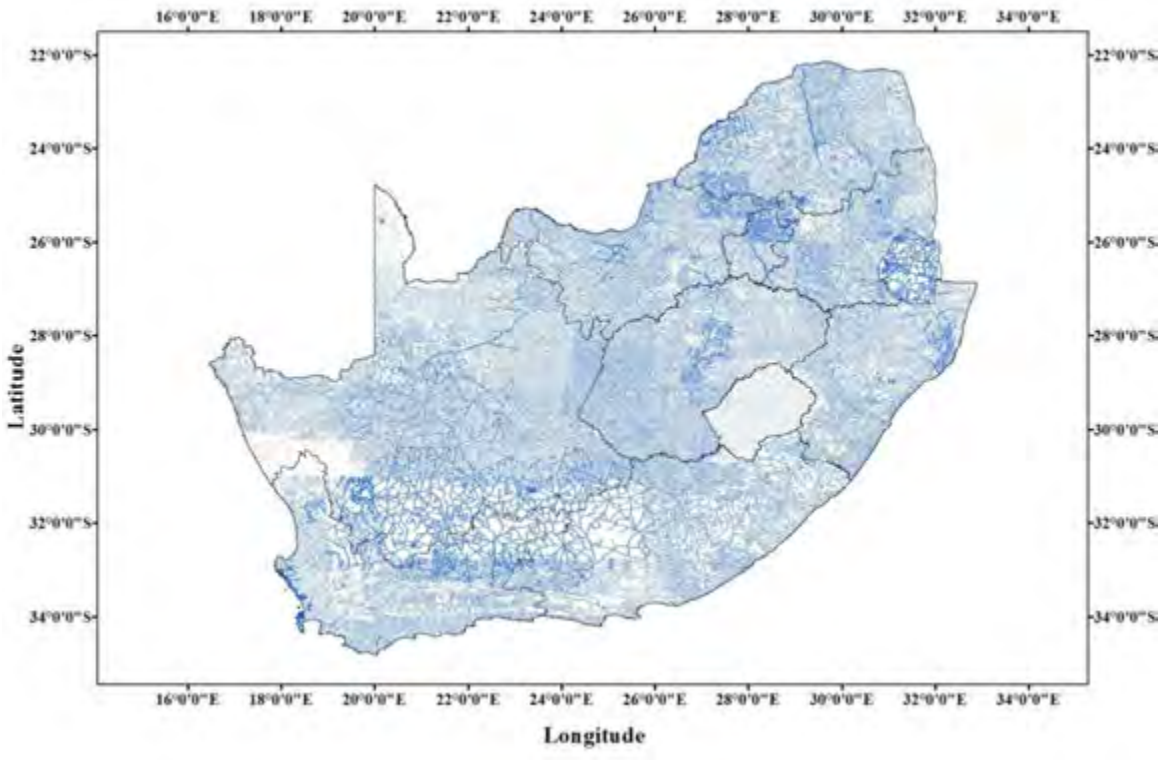

Figure 4-2 Density of the gravity data set over South Africa

5 RESULTS AND ANALYSIS

The gravimetric geoid models were computed over the region of Gauteng province, bound with $-28°0'0"$ $-24\ 0\ 0$ and $26\ 0\ 0" \leq \lambda \leq 30°0'0"$. The input grids are extended by 1° beyond the study area to reduce the edge effects. Two geoid models were computed in this research, SiPLSC and SiPFFT geoid model, using spherical harmonic coefficients from the EGM2008 geopotential model complete to an order and degree 720.

A $0.3^o \times 0.3^o$ grid was used for computation of the local geoid model over the study area. There were 1853 gravity data points distributed over the region of Gauteng province; the geoidal heights were computed at each data point. The figure (5-1) below depicts the distribution of gravity data points over the study:

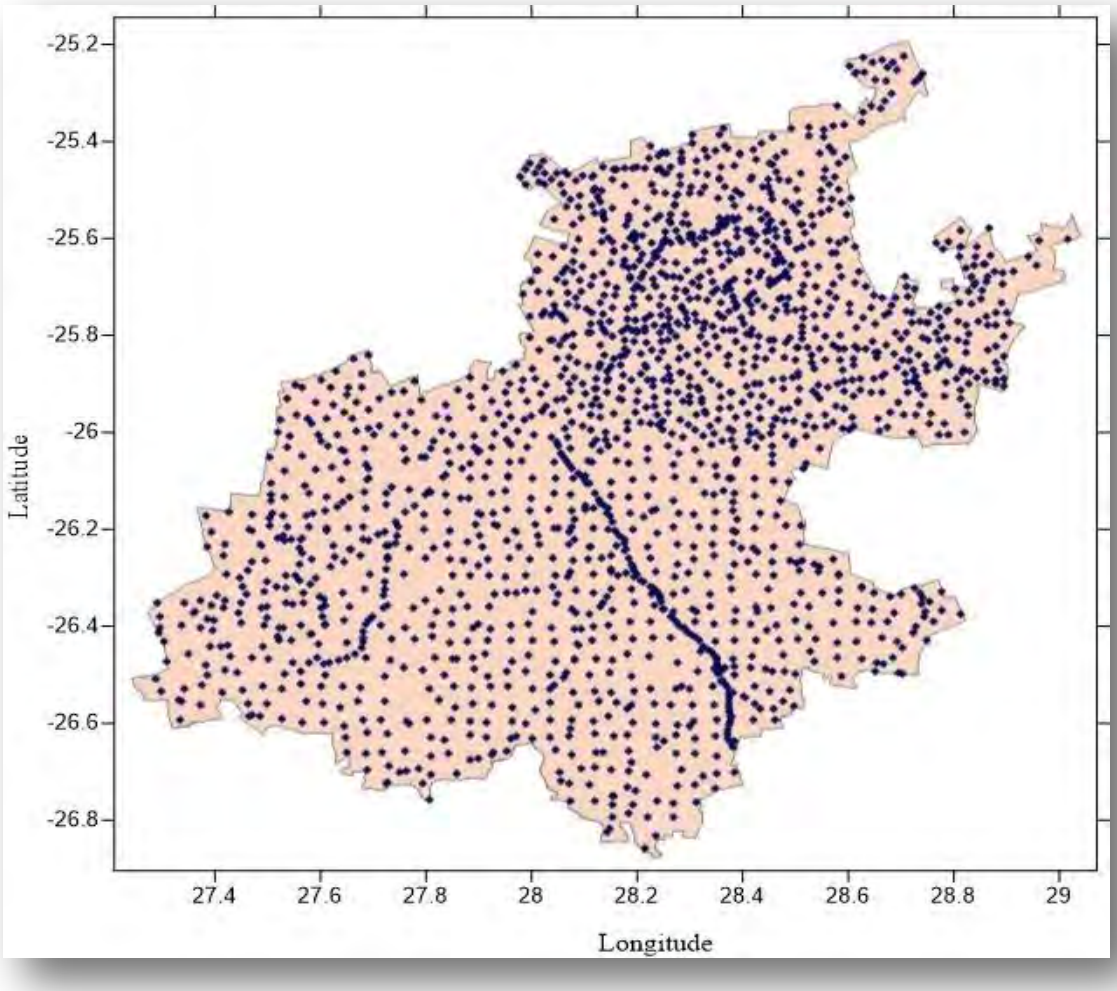

Figure 5-1: Distribution of gravity data points over Gauteng province.

The SiPLSC geoid model was computed using the least squares collocation method and the SiPFFT geoid model was computed using the one dimensional FFT method. Refer to appendix C and D for more detailed statistics report. The statistical results of the two geoid models are as illustrated on the table (5-1) below:

Table 5-1: Statistics results of the SiPLSC and SiPFFT geoid models

Model	Min. (m)	Max. (m)	Mean (m)	Std. Dev. (m)	RMS (m)
SiPLSC	20.697	28.946	25.929	1.681	25.983
SiPFFT	20.660	28.910	25.892	1.681	25.946

It is observed from the table (5-1) above that the two approaches used for evaluating Stokes' integral are consistent. The least squares collocation technique allows the consistent treatment of heterogeneous gravity data. It requires an excessive amount of computer time when working with large data set. It is a multiple-input-single-output method. Due to the increase of data size and quality, a more reliable and efficient technique has been required.

The FFT technique produces the same results as the least squares collocation for geoid model computation. The FFT approach differs from the least squares collocation in that it uses regular grid data and can handle a large amount of data in one run. The FFT technique has become a standard procedure for geoid computation. The figure (5-2) below depicts a 0.5m interval contour plot of the SiPFFT geoid model over the study area.

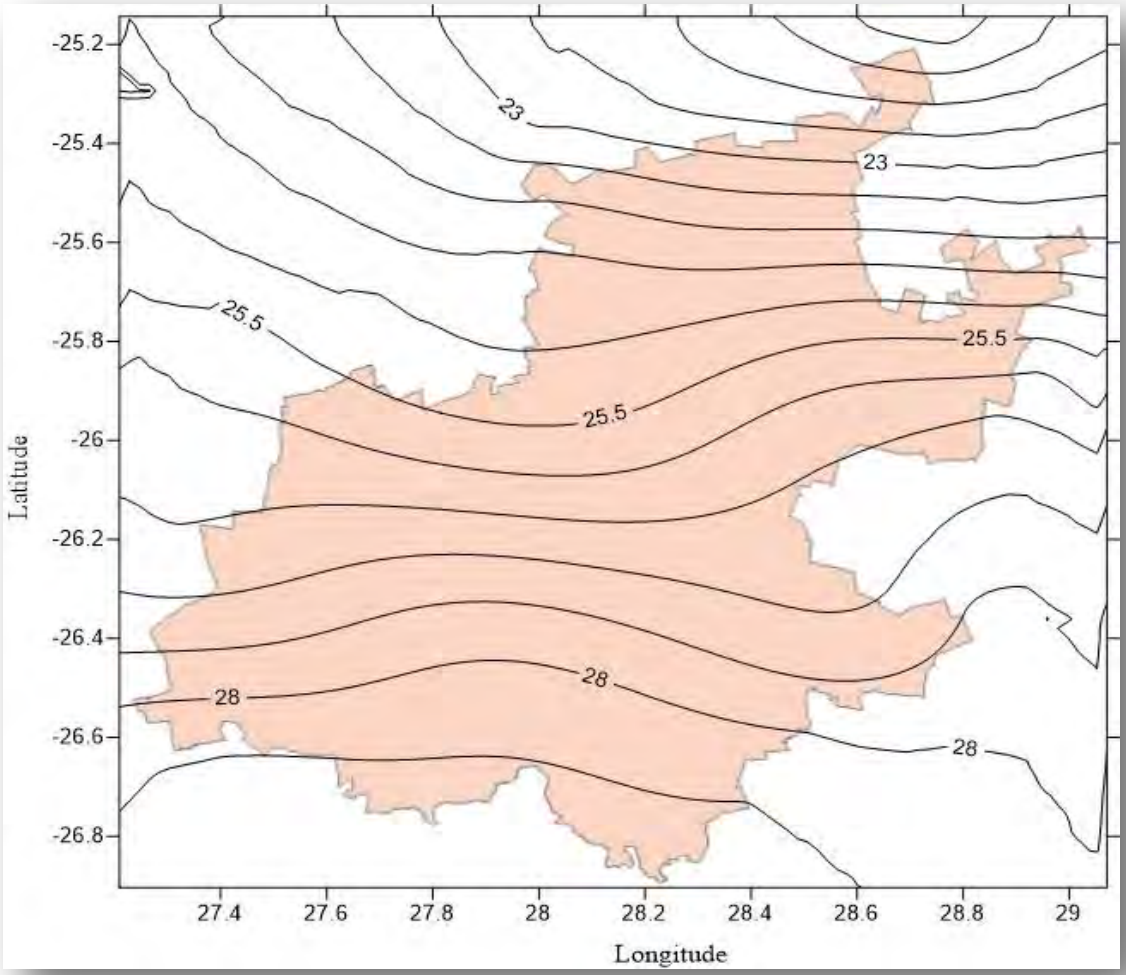

Figure 5-2: SiPFFT geoid model at 0.5m interval contour plot.

The computed geoid model over the region of Gauteng province seems to be gradually increasing towards the south west part of the province. Refer to appendix E for more detailed statistics report. The consistency of the results between the two techniques is as illustrated by the statistical results on the table (5-2) below:

Table 5-2: Comparison of the SiPLSC and the SiPFFT geoid model.

Comparison	Min. (m)	Max. (m)	Mean (m)	Std. Dev. (m)	RMS (m)
SiPLSC-SiPFFT	0.036	0.037	0.037	0.000	0.037

The computed geoid models were not compared to GPS/levelling data due to the lack of data over the study area. Refer to appendix G and H for more detailed statistics report. The

comparison of the computed geoid models with the SAGEOID10 hybrid-geoid model over the study area is as illustrated by the statistical results on the table (5-3) below:

Table 5-3: Comparison of the computed geoid models with the SAGEOID10 hybrid geoid model.

Comparison	Min. (m)	Max. (m)	Mean (m)	Std. Dev. (m)	RMS (m)
SiPLSC- SAGEOID10	-0.254	0.147	-0.039	0.056	0.069
SiPFFT- SAGEOID10	-0.290	0.110	-0.076	0.056	0.094

The long wavelength component of the computed geoid model was compared to the geoidal height interpolated in a grid of values for the earth gravity model, EGM2008. An online version of the GeoidEval (version 1.46) software was used, available at *(http://geographiclib.sourceforge.net/cgi-bin/GeoidEval)*. The RMS error in the interpolated geoidal height is about 1.0mm (Karnely, 2009). Only 39 random data points were selected for this comparison. Refer to appendix F for more detailed statistics report. The results of the comparison are as illustrated on the table (5-4) below:

Table 5-4: Comparing the long wavelength component of the computed geoid model to the interpolated geoidal height from the full EGM2008 geopotential model.

Comparison	Min. (m)	Max. (m)	Mean (m)	Std. Dev. (m)	RMS (m)
Long wavelength comp.- EGM2008	0.133	0.288	0.198	0.042	0.202

The full EGM2008 geopotential model refers to the spherical harmonic coefficients of the EGM2008 model complete to degree and order 2160. The computed long wavelength component is computed using spherical harmonic coefficients of the EGM2008 geopotential model truncated at degree 720. This might have caused the existing discrepancies.

5.1 Errors involved with the ellipsoidal, geoidal and orthometric height

The relationship that binds the ellipsoidal heights obtained from GPS measurements and heights with respect to a vertical datum established from spirit-levelling (orthometric height) and gravity data is given by equation (1:1) above.

The existing systematic distortions between the geometric geoidal height and the gravimetric geoidal height can be modelled using a four parametric mathematical model. The

mathematical model is used as a surface fit/correction surface to reduce existing distortions between the geometric geoidal height and the gravimetric geoidal height. The existing offset between the local geoid model and the GPS/levelling data can be computed as follow (Kiamehr, 2006):

$$N^{GPS/levelling} - N^{GM} = h - H - N^{GM} \qquad (5:1)$$
$$= x_0 + x_1 \cos\varphi \cos\lambda + x_2 \cos\varphi \sin\lambda + x_3 \sin\varphi,$$

Where:-

$N^{GPS/levelling}\ and\ N^{GM}$ – Represent a geometric geoidal height and a gravimetric geoidal height,

$x_0, x_1, x_2, and\ x_3$ – Represent the four unknown parameters,

$\varphi\ and\ \lambda$ – Geodetic latitude and longitude of the computation point,

$h\ and\ H$ – Represent the orthometric and the ellipsoidal height.

The solution of the unknown parameters can be determined using least squares method. The correction surface was not computed in this study due to the lack of GPS/ levelling data over the study area. There are a number of factors which contributes to this offset; few of these factors are mentioned as follow (Kotsakis & Sideris, 1999):

i. Random errors resulting from heights h, H, and N.
ii. Systematic effects and distortions caused by long-wavelength geoid errors such as poorly modelled GPS errors (e.g. tropospheric refraction),
iii. Over constrained adjustment of the levelling network datum,
iv. Inconsistencies inherent among the height types (h, H, and N), each of which usually refers to a slightly different reference surface.
v. Assumptions and theoretical approximations made in processing data, such as neglecting sea surface topography effects or river discharge corrections for measured tide gauge values.
vi. Movement of the reference station over time because of geodynamic effects (such as, post-glacial rebound, land subsidence, plate deformation near subduction zones, mean sea level rise, monument instabilities).

6 CONCLUSIONS AND FINDINGS

The effect of using the least squares collocation and 1D-FFT technique for a gravimetric geoid model computation over the region of Gauteng province has been studied in this research.

The geoid solution by the least squares collocation and the 1D-FFT technique differ from each other on average by 3.7cm. The long wavelength component of the computed geoid model compared to the full EGM2008 geopotential model with a standard deviation of 4.2cm, only 39 random data points were used for this comparison. This comparison was only done to validate the computed long wavelength component of the computed geoid model.

The 1D-FFT technique is the best geoid determination technique due to an increase in data density and distribution. It handles a large amount of data in one run. The FFT technique has become a standard procedure for geoid computation, particularly for computational efficiency.

The computed geoid model was not corrected for systematic distortions due to the lack of GPS/levelling data over the region of Gauteng province. The GPS/levelling data points and the gravity data need to be intensified to improve the quality of the computed geoid model. This is also necessary to provide improvements on the quality of the vertical datum of South Africa, since the geoid based vertical datum is defined more by geoid modelling than measurements.

The computed geoid models illustrate the agreement with the SAGEOID10 hybrid geoid model with standard deviation of 5.6cm. The SiPLSC geoid model seems to be closer to the SAGEOID10 hybrid geoid model than the SiPFFT geoid model.

The SAGEOID10 is the South African hybrid geoid which was developed for transforming GPS derived ellipsoidal heights to orthometric heights on the LLD. However, the accuracy of the orthometric height determined from the conversion depends on the quality of the geoid model and the ellipsoidal height derived from the GNSS system. The precise hybrid geoid model SAGEOID10 was developed for the Chief Directorate: National Geospatial Information (CD: NGI).

Maintaining temporal stability for the local geoid model, it should not be updated too frequently, for instance, immediately after a new model is available. The levelling databases

should be acknowledged also since it will still be useful for validating and evaluation of geoid models, and for other scientific studies. The use of the GNSS system reduces occupation time for surveying techniques.

REFERENCES

Akib, W.M. & Aziz, W.A. 1996. The Use of FFT Method in Geoid Modelling. *Buletin Ukur.* 7(2).

Alberts, B. & voor Geodesie, N.C. 2009. *Regional gravity field modeling using airborne gravimetry data.* NCG, Nederlandse Commissie voor Geodesie.

Altamimi, Z., Collilieux, X., Legrand, J., Garayt, B. & Boucher, C. 2007. ITRF2005: A new release of the International Terrestrial Reference Frame based on time series of station positions and Earth Orientation Parameters. *Journal of Geophysical Research: Solid Earth (1978–2012).* 112(B9).

Amos, M. & Featherstone, W. 2009. Unification of New Zealand's local vertical datums: iterative gravimetric quasigeoid computations. *Journal of Geodesy.* 83(1):57-68.

Barthelmes, F. 2009. Definition of functionals of the geopotential and their calculation from spherical harmonic models. *Deutsches Geo-ForschungsZentrum GFZ.*

Beheshti, A. & Kiamehr, R. 2008. Overview of geodynamical patterns over Iran based on the garadiametry by EGM 2008 global geopotential model.

Blitzkow, D., Matos, A., Guimarães, G. & Lobianco, M. 2010. Recent progress of the geoid in South America. *Presentado En La Reunión SIRGAS.*

Brown, N., Featherstone, W. & Hu, G.2010. AUSGeoid09: Improving the access to Australia's vertical datum. *XXIV FIG International Congress.* 11.

Chandler, G. & Merry, C. 2010. The South African geoid 2010: SAGEOID10. *Position IT.* :29-33.

Chen, Y. & Yang, Z.2001. A hybrid method to determine the Hong Kong geoid. *Fédération International Des Géomètres Conference "New Technology for a New Century", Seoul.*

Childers, V., Smith, D., Roman, D., Diehl, T. & Eckl, M.2009. NGS'GRAV-D Project: Current update and future prospects. *AGU Fall Meeting Abstracts.* 04.

Claessens, S.J., Hirt, C., Amos, M., Featherstone, W. & Kirby, J. 2011. The NZGEOID09 model of New Zealand. *Survey Review.* 43(319):2-15.

Claessens, S., Hirt, C., Featherstone, W. & Kirby, J. 2009. *Computation of a New Gravimetric Quasigeoid Model for New Zealand.*

Craymer, M., Ferland, R. & Snay, R. 2000. Realization and Unification of NAD83 in Canada and the US via the ITRF. In *Towards an integrated global geodetic observing system (IGGOS).* Springer. 118-121.

Decker, B.L. 1986. *World Geodetic System 1984.*

Drewes, H., Hornik, H., Ádám, J. & Rózsa, S. 2012. The geodesist's handbook 2012. *J Geod.* 86:49-51.

Drewes, H., Hornik, H., Ádám, J. & Rózsa, S. 2012. Journal of Geodesy. *Journal of Geodesy.* 86(10):787-974.

Engelis, T., Rapp, R.H. & Tscherning, C. 1984. The precise computation of geoid undulation differences with comparison to results obtained from the Global Positioning System. *Geophysical Research Letters.* 11(9):821-824.

Featherstone, W. 2000. Towards the unification of the Australian height datum between the mainland and Tasmania using GPS and AUSGeoid98. *Geomatics Research Australasia.* :33-54.

Featherstone, W., Filmer, M., Claessens, S., Kuhn, M., Hirt, C. & Kirby, J. 2012. Regional geoid-model-based vertical datums–some Australian perspectives. *Journal of Geodetic Science.* 2(4):370-376.

Featherstone, W. & Kirby, J. 2000. The reduction of aliasing in gravity anomalies and geoid heights using digital terrain data. *Geophysical Journal International.* 141(1):204-212.

Featherstone, W., Kirby, J., Kearsley, A., Gilliland, J., Johnston, G., Steed, J., Forsberg, R. & Sideris, M. 2001. The AUSGeoid98 geoid model of Australia: data treatment, computations and comparisons with GPS-levelling data. *Journal of Geodesy.* 75(5-6):313-330.

Featherstone, W. & Kuhn, M. 2006. Height systems and vertical datums: a review in the Australian context. *Journal of Spatial Science.* 51(1):21-41.

Featherstone, W. 1998. Do we need a gravimetric geoid or a model of the Australian Height datum to transform GPS Heights in Australia? *Australian Surveyor.* 43(4):273-280.

Fecher, T., Pail, R. & Gruber, T. 2015. Global gravity field modeling based on GOCE and complementary gravity data. *International Journal of Applied Earth Observation and Geoinformation.* 35:120-127.

Filmer, M. & Featherstone, W. 2012. Three viable options for a new Australian vertical datum. *Journal of Spatial Science.* 57(1):19-36.

Forsberg, R. & Tscherning, C. 1981. The use of height data in gravity field approximation by collocation. *Journal of Geophysical Research: Solid Earth (1978–2012).* 86(B9):7843-7854.

Förste, C., Bruinsma, S., Abrikosov, O., Flechtner, F., Marty, J., Lemoine, J., Dahle, C., Neumayer, H. et al.2014. EIGEN-6C4-The latest combined global gravity field model including GOCE data up to degree and order 1949 of GFZ Potsdam and GRGS Toulouse. *EGU General Assembly Conference Abstracts.* 3707.

Förste, C., Flechtner, F., Schmidt, R., König, R., Meyer, U., Stubenvoll, R., Rothacher, M., Barthelmes, F. et al.2006. Global mean gravity field models from combination of

satellite mission and altimetry/gravimetry surface data. *Proceedings of the 3rd International GOCE User Workshop, Frascati, Italy,(ESA SP-627.* 6.

Fotopoulos, G., Kotsakis, C. & Sideris, M.G. 1999. *Evaluation of Geoid Models and Their Use in Combined GPS Levelling, Geoid Height Network Adjustments.* Univ.

Fotopoulos, G. 2003. *An analysis on the optimal combination of geoid, orthometric and ellipsoidal height data.* Citeseer.

Gilardoni, M., Reguzzoni, M. & Sampietro, D. 2016. GECO: a global gravity model by locally combining GOCE data and EGM2008. *Studia Geophysica Et Geodaetica.* :1-20.

Gill, S.K. & Schultz, J.R. 2001. *Tidal datums and their applications.* National Oceanic and Atmospheric Administration.

Graham, K. & Hales, A. 1965. Surface-ship gravity measurements in the Agulhas bank area, south of South Africa. *Journal of Geophysical Research.* 70(16):4005-4011.

Heiskanen, W.A. & Moritz, H. 1967. Physical geodesy. *Bulletin Géodésique (1946-1975).* 86(1):491-492.

Heitz, S. & Tscherning, C. 1972. Comparison of two methods of astrogeodetic geoid determination based on least squares prediction and collocation. *Tellus.* 24(3):271-276.

Hofmann-Wellenhof, B., Lichtenegger, H. & Wasle, E. 2007. *GNSS–global navigation satellite systems: GPS, GLONASS, Galileo, and more.* Springer.

Hofmann-Wellenhof, B. & Moritz, H. 2005. *Physical geodesy.* Springer.

Holmes, S.A. & Featherstone, W.E. 2002. A unified approach to the Clenshaw summation and the recursive computation of very high degree and order normalised associated Legendre functions. *Journal of Geodesy.* 76(5):279-299.

Hooijberg, M. 2012. *Practical Geodesy: Using Computers.* Springer Science & Business Media.

Hwang, C. 1998. Inverse Vening Meinesz formula and deflection-geoid formula: applications to the predictions of gravity and geoid over the South China Sea. *Journal of Geodesy.* 72(5):304-312.

Jiang, Z. & Duquenne, H. 1996. On the combined adjustment of a gravimetrically determined geoid and GPS levelling stations. *Journal of Geodesy.* 70(8):505-514.

Katz, V.J. 1979. The history of Stokes' theorem. *Mathematics Magazine.* :146-156.

Keysers, J.H., Quadros, N.D. & Collier, P.A. 2013. Vertical Datum Transformations across the Australian Littoral Zone. *Journal of Coastal Research.*

Kiamehr, R. 2006. Precise Gravimetric Geoid Model for Iran Based on GRACE and SRTM Data and the Least-Squares Modification of Stokes' Formula: with Some Geodynamic Interpretations.

Kotsakis, C. & Sideris, M.G. 1999. On the adjustment of combined GPS/levelling/geoid networks. *Journal of Geodesy.* 73(8):412-421.

Lemoine, F., Zelensky, N., Chinn, D., Pavlis, D., Rowlands, D., Beckley, B., Luthcke, S., Willis, P. et al. 2010. Towards development of a consistent orbit series for TOPEX, Jason-1, and Jason-2. *Advances in Space Research.* 46(12):1513-1540.

Lemoine, F.G., Kenyon, S.C., Factor, J.K., Trimmer, R.G., Pavlis, N.K., Chinn, D.S., Cox, C.M., Klosko, S.M. et al. 1998. The development of the joint NASA GSFC and the National Imagery and Mapping Agency (NIMA) geopotential model EGM96.

Li, F., YUE, J. & ZHANG, L. 2005. Determination of geoid by GPS/Gravity data. *Chinese Journal of Geophysics.* 48(2):326-330.

Losch, M. & Seufer, V. 2003. How to Compute Geoid Undulations (Geoid Height Relative to a Given Reference Ellipsoid) from Spherical Harmonic Coefficients for Satellite Altimetry Applications. *Http://mitgcm.Org/~ mlosch/geoidcookbook/geoidcookbook.Html.*

Marti, U.2007. Comparison of high precision geoid models in Switzerland. *Dynamic Planet.* Springer. 377.

Martinec, Z. & Vanicek, P. 1994. The indirect effect of topography in the Stokes-Helmert technique for a spherical approximation of the geoid. *Manuscripta Geodaetica.* 19(4):213-219.

Merry, C.L. 2007. Evaluation of global geopotential models in determining the quasi-geoid for Southern Africa. *Survey Review.* 39(305):180-192.

Merry, C.2003. The African geoid project and its relevance to the unification of African vertical reference frames. *Proceedings of the 2nd FIG Regional Conference.*

Merry, C., Blitzkow, D., Abd-Elmotaal, H., Fashir, H., John, S., Podmore, F. & Fairhead, J. 2005. A preliminary geoid model for Africa. In *A Window on the Future of Geodesy.* Springer. 374-379.

Moritz, C. 1972. *Current Biography Yearbook, 1971.* HW wilson Company.

Moritz, H. 1972. *Advanced least-squares methods.* Department of Geodetic Science, Ohio State University Columbus.

Moritz, H. 1978. Least-squares collocation. *Reviews of Geophysics.* 16(3):421-430.

Moritz, H. 1978. Least-squares collocation. *Reviews of Geophysics.* 16(3):421-430.

Moritz, H. 1980. Advanced physical geodesy. *Karlsruhe: Wichmann; Tunbridge, Eng.: Abacus Press, 1980.* 1.

Murphy, C.A.2004. The Air-FTG airborne gravity gradiometer system. *Airborne Gravity 2004–Abstracts from the ASEG-PESA Airborne Gravity 2004 Workshop: Geoscience Australian Record.* 7.

Parker, A., Merry, C., Combrinck, W., Combrink, A. & Wonnacott, R. 2011. *Review of Recent Research in Geodesy in South Africa: 2003–2006.*

Pavlis, N.K., Holmes, S.A., Kenyon, S.C. & Factor, J.K. 2008. An earth gravitational model to degree 2160: EGM2008. *EGU General Assembly.* :13-18.

Ramjattan, A.N. & Cross, P.A. 1995. A Kalman filter model for an integrated land vehicle navigation system. *Journal of Navigation.* 48(02):293-302.

Ray, J., Dong, D. & Altamimi, Z. 2004. IGS reference frames: status and future improvements. *GPS Solutions.* 8(4):251-266.

Rodríguez-Caderot, G., Lacy, M., Gil, A. & Blazquez, B. 2006. Comparing recent geopotential models in Andalusia (Southern Spain). *Studia Geophysica Et Geodaetica.* 50(4):619-631.

Roman, D. & Weston, N.D. 2012. Beyond GEOID12: implementing a new vertical datum for North America. *FIG Proceedings.*

Roman, D.R., Wang, Y.M., Saleh, J. & Li, X.2009. National geoid height models for the United States: USGG2009 and GEOID09. *Proceedings of the ACSM-MARLS-UCLS-WFPS Conference, Salt Lake City, UT, USA.* 20.

ROMAN, D.R., WANG, Y.M., SALEH, J. & LI, X.2010. Geodesy, geoids, and vertical datums: A perspective from the US National Geodetic Survey. *FIG Congress.* 11.

ROMAN, D.R., WANG, Y.M., SALEH, J. & LI, X.2010. Geodesy, geoids, and vertical datums: A perspective from the US National Geodetic Survey. *FIG Congress.* 11.

Roman, D.R. & Weston, N.D.2012. Beyond GEOID12: Implementing a New Vertical Datum for North America. *Proceedings of the FIG Working Week.* 6.

Sander, S., Argyle, M., Elieff, S., Ferguson, S., Lavoie, V. & Sander, L.2004. The AIRGrav airborne gravity system. *Airborne Gravity 2004 Workshop, Sydney, Australia.*

Schwarz, K., Sideris, M. & Forsberg, R. 1987. Orthometric heights without leveling. *Journal of Surveying Engineering.* 113(1):28-40.

Schwarz, K., Sideris, M. & Forsberg, R. 1990. The use of FFT techniques in physical geodesy. *Geophysical Journal International.* 100(3):485-514.

Sideris, M. & Tziavos, I. 1988. FFT-evaluation and applications of gravity-field convolution integrals with mean and point data. *Bulletin Géodésique.* 62(4):521-540.

Sideris, M.G. 2013. Geoid determination by FFT techniques. In *Geoid Determination.* Springer. 453-516.

Sideris, M.G. & She, B.B. 1995. A new, high-resolution geoid for Canada and part of the US by the 1D-FFT method. *Bulletin Géodésique.* 69(2):92-108.

Sledzinski, J.2005. Application of Satellite Navigation Systems in Geodetic and Geodynamic Programmes of the CEI. *Report on the Symposium of the IAG Sub-Commission for Europe (EUREF) Held in Bratislava, 2-5 June 2004: Reports of the EUREF Technical Working Group (TWG).* Verlag des Bundesamtes für Kartographie und Geodäsie. 385.

Smith, D. 2007. The GRAV-D project: gravity for the redefinition of the American Vertical Datum. *NOAA Website: Http://www.Ngs.Noaa.gov/GRAV-D/pubs/GRAV-D_v2007_12_19.Pdf.*

Smith, D., Véronneau, M., Roman, D., Huang, J., Wang, Y. & Sideris, M. 2013. Towards the unification of the vertical datum over the North American continent. In *Reference Frames for Applications in Geosciences.* Springer. 253-258.

Soycan, M. & Soycan, A. 2003. Surface modeling for GPS-levelling geoid determination. *Newton's Bulletin.* 1:41-52.

Torge, W. 2001. *Geodesy.* Walter de Gruyter.

Tschernig, C. & Arabelos, D. 2005. Computation of a geopotential model from GOCE data using fast spherical collocation—a simulation study. In *A Window on the Future of Geodesy.* Springer. 310-313.

Tscherning, C. Least-Squares Collocation. .

Tscherning, C. 1994. Geoid determination by least-squares collocation using GRAVSOFT. *Lecture Notes for the International School for the Determination and use of the Geoid, Milan, October.*

Ulotu, P. 2009. Geoid model of Tanzania from sparse and varying gravity data density by the KTH method.

van Gelderen, M. 1991. *The geodetic boundary value problem in two dimensions and its iterative solution.* Nederlandse Commissie voor Geodesie.

Vanicek, P. 1991. Vertical datum and NAVD88. *Surveying and Land Information Systems.* 51(2):83-86.

Vella, J. & Featherstone, W. 1999. A gravimetric geoid model of Tasmania, computed using the one-dimensional fast Fourier transform and a deterministically modified kernel. *Geomatics Research Australasia.* :53-76.

Weston, N.D., Schwieger, V. & International Federation of Surveyors. FIG Commission 5 2010. *Cost effective GNSS positioning techniques.* International Federation of Surveyors (FIG).

Wonnacott, R.; Merry, C. (2011). A New Vertical Datum for South Africa?, In Conference Proceedings of the AfricaGEO.

Wonnacott, R. 1999. The Implementation of the Hartebeesthoek94 Co-ordinate System in South Africa. *Survey Review.* 35(274):243-250.

Yun, H. 1999. Precision geoid determination by spherical FFT in and around the Korean peninsula. *Earth Planets and Space.* 51(1):13-18.

Zilkoski, D.B. 1992. Special Report Results of the General Adjustment of the North American Vertical Datum of 1988 David B. Zilkoski, John H. Richards, and Gary M. Young. *Surveying and Land Information Systems.* 52(3):133-149.

Web-Pages:

1. Natural Resource Canada. Retrieved 28 March 2014, from http://www.nrcan.gc.ca/earth-sciences/geomatics/geodetic-reference-systems/tools-applications/9070
2. Zilkoski , 2015 , Retrieved: March 2016, http://gpsworld.com/establishing-orthometric-heights-using-gnss-part-3/
3. National Geodetic Survey (NGS), Retrieved: February 2016, http://www.ngs.noaa.gov/GEOID/GEOID12B/GEOID12B_TD.shtml

APPENDIX A

Boundary value problem

The spherical harmonics for the global approach and the gravity reduction by an integral equation for the local studies, all in a compatible system, give a solution of the principal boundary value problem of physical geodesy (Bjerhammar, 1969). Stokes (1849) solved the boundary value problem for physical geodesy for a sphere.

The fundamental equation of physical geodesy relates the measured quantity of gravity anomaly (Δg) to the unknown disturbing potential T. This relationship is expressed in the following form (Heiskanen and Moritz, 1967):

(a)

Where:-

Elevation of a point,

Gravity anomaly at the point,

Disturbing potential,

Normal gravity at the point,

The above equation (2:1) can be solved as the partial differential equation if the gravity anomalies were known at every point on the surface of the earth. The gravity anomaly is known only along the geoid surface (Heiskanen and Moritz, 1967). The gravity observations are not directly measured on the geoid; they are measured on the physical surface of the earth then reduced to the geoid. The fundamental equation (2:1) is used only as a boundary condition which alone is not sufficient for computing the disturbing potential (Heiskanen and Moritz, 1967).

The disturbing potential is harmonic and satisfies Laplace's equation, that is when there is no mass everywhere outside the geoid. The effect of masses outside the geoid is removed, so it is assumed that all masses are enclosed by the geoid (Heiskanen and Moritz, 1967). The partial differential equation is sufficient for computing T at every point outside the geoid; it can be expressed by the Laplace's equation as shown below (Heiskanen and Moritz, 1967):

$$\nabla^2 T = 0.$$

$$\Delta T \equiv \frac{\partial^2 T}{\partial x^2} + \frac{\partial^2 T}{\partial y^2} + \frac{\partial^2 T}{\partial z^2} = 0. \quad \text{(b)}$$

The computation of T defines a third boundary value problem of potential theory which is particularly relevant to physical geodesy. Furthermore, this relationship can derive from Poisson's integral for harmonic parameters, as expressed below (Bjerhammar, 1969):

$$r_j \Delta g_j = \frac{r_j^2 - R^2}{4\pi r_j} \iint \frac{\Delta g^*}{r_{ij}^3} dS \quad \text{(c)}$$

Where:-

$r_j -$ Local ellipsoidal radius for a specific data point,

$\Delta g_j -$Free air gravity anomaly at the fixed point,

$R -$ Mean radius of the earth,

$S -$ Surface of the reference sphere,

$r_{ij} -$ Distance between the fixed point P_j and the moving point at the reference sphere,

$\Delta g^* -$ Gravity at the reference sphere.

This can be expressed using Legendre polynomials as follow (Bjerhammar, 1969):

$$\Delta g_j = \frac{1}{4\pi r_j^2} \iint \Delta g^* \sum_{n=0}^{n_{max}} (2n+1) \left(\frac{R}{r_j}\right)^n P_n(\cos\psi)\, dS \quad \text{(d)}$$

Where:-

$\psi -$ Angular distance,

$P_n(\cos\psi) -$ Legendre polynomial of order n,

The final solution of the disturbing potential is now expressed follow:

$$T_j = \frac{1}{4\pi r_j} \iint \Delta g^* \sum_{n=2}^{n_{max}} \frac{2n+1}{n-1} \left(\frac{R}{r_j}\right)^n P_n(\cos\psi)\, dS \quad \text{(e)}$$

Where:-

$T_j -$ Disturbing potential of the fixed point P_j

The disturbing potential is defined by the integral of the Stokes' integral, equation (2:4) can further be expressed as follow (Bjerhammar, 1969):

$$T_j = \frac{1}{4\pi r_j} \iint \Delta g^* . S(\psi)\, dS \tag{f}$$

The conditions expressed on the above equations (2:1) and (2:2) are fulfilled for this solution. The disturbing potential can expanded using spherical harmonic coefficients. In this case the Laplace condition must be valid also between the reference ellipsoid and the physical surface. The geoidal undulation (N) can be computed from the T using the Bruns' formula (Heiskanen and Moritz, 1967), can be expressed as follow:

$$N = \frac{T}{\gamma}. \tag{g}$$

APPENDIX B

The following is the list of the source code of the gravity data used in this research for the geoid model computation:

i. **University, Research and Commercial Organisations in Africa:**

01 University of Cape Town
02 University of Zimbabwe - removed Nov. 2000
03 CSIR, Pretoria
04 Gencor
05 Geodass
06 Poseidon Geophysics

ii. **Government Departments in Africa:**

11 Geological Survey of South Africa
12 Surveys & Mapping Directorate, South Africa
13 Geological Survey of Botswana
14 Geological Survey of Zambia
15 Geological Survey of Zimbabwe, Bulletin 103
16 Geological Survey of South Africa, October 1997 data set
17 Geological Survey of Namibia
18 Geological Survey of South Africa May 1999 supplement

iii. **International Organisations**

21 International Association of Geodesy
22 Bureau Gravimetrique International
23 Defense Mapping Agency, USA
24 Institute of Geological Sciences, London
25 Woods Hole Oceanographic Institute
26 Ministerio do Ultramar, Portugal
27 National Geophysical Data Centre, USA
28 512 STRE, UK Department of Defense - removed Nov. 2000
29 Defense Mapping Agency, second data set
30 African Gravity Project, Univ. of Leeds - open file
31 African Gravity Project, Univ. of Leeds - restricted data

The format of the gravity data file:

Each record consists of the following fields; they are as listed below in more detail:

Source code:	2 digit integer code for source of gravity data
Station name:	10 character station name (in many cases, this is just a sequence number).
Latitude:	10 character decimal degrees (six decimal places); negative

	south of the equator.
Longitude:	10 character decimal degrees (six decimal places); positive east of Greenwich.
Position accuracy:	5 characters, metres, 1 decimal place. In most cases this is no more than a rough estimate.
Height:	8 character, metres, 2 decimal places. Height above mean sea level (orthometric height). Negative for depths below sea level.
Height accuracy:	5 character, metres, 2 decimal places. In most cases this is no more than a rough estimate.
Gravity:	9 character, mgals, 2 decimal places. IGSN71 system.
Gravity accuracy:	5 character, mgals, 2 decimal places. In most cases this is no more than a rough estimate.
Free-air gravity anomaly:	7 character, mgals, 2 decimal places. Gradient of 0.3086 mgals per metre. Corrected for the effect of the atmosphere.
Bouguer anomaly:	7 character, mgals, 2 decimal places. Gradient of 0.1967 mgals per metre. Corrected for the effect of the atmosphere. Identical to the free-air anomaly at sea.

Each field is separated from the next by means of a single space.

Example:

```
18 ecape3884  -32.805833  26.743611  30.0   571.00  5.00 979369.69  0.20   -3.49  -67.38

123456789012345678901234567890123456789012345678901234567890123456789012345678
```

APPENDIX C

Data Statistics Report

Thu May 05 06:01:55 2016

Data Source

Source Data File Name:	C:\Users\Siphiwe\Desktop\Processing-data\comp.Geoid-data\Geoidlscx.dat
X Column:	A
Y Column:	B
Z Column:	C

Data Counts

Active Data:	1853

Original Data:	1853
Excluded Data:	0
Deleted Duplicates:	0
Retained Duplicates:	0
Artificial Data:	0
Superseded Data:	0

Exclusion Filtering

Exclusion Filter String:	Not In Use

Duplicate Filtering

Duplicate Points to Keep:	First
X Duplicate Tolerance:	2E-007
Y Duplicate Tolerance:	2.2E-007

No duplicate data were found.

Breakline Filtering

Breakline Filtering:	Not In Use

Data Counts

Active Data:	1853

Univariate Statistics

	X	Y	Z
Count:	1853	1853	1853
1%%-tile:	-26.777222	27.298889	21.55266007
5%%-tile:	-26.64	27.466389	23.04968211
10%%-tile:	-26.549167	27.592222	23.68214571
25%%-tile:	-26.341667	27.97	24.80069435
50%%-tile:	-25.962778	28.23	25.97297324
75%%-tile:	-25.699167	28.458056	27.30158607
90%%-tile:	-25.507778	28.678333	28.14859054
95%%-tile:	-25.41	28.791944	28.46347089
99%%-tile:	-25.253889	28.923333	28.75018366
Minimum:	-26.903889	27.209167	20.69748534
Maximum:	-25.143889	29.071111	28.94654526
Mean:	-26.0084655618	28.1878346001	25.9289730945
Median:	-25.962778	28.23	25.97297324
Geometric Mean:	N/A	28.1851342443	25.8734151044
Harmonic Mean:	N/A	28.1824242413	25.8167343716
Root Mean Square:	26.0114032493	28.1905252085	25.9833910968
Trim Mean (10%%):	-26.0069829215	28.194846964	25.9784941466
Interquartile Mean:	-25.9929342071	28.225078219	25.9999657474
Midrange:	-26.023889	28.140139	24.8220153
Winsorized Mean:	-26.0091646287	28.1894760281	25.9805655377
TriMean:	-25.9915975	28.222014	26.012056725
Variance:	0.152900634502	0.151773997064	2.82649251168
Standard Deviation:	0.391025107253	0.389581823323	1.68121756822
Interquartile Range:	0.6425	0.488056	2.50089172
Range:	1.76	1.861944	8.24905992
Mean Difference:	0.449728721895	0.440241595816	1.91322918866
Median Abs. Deviation:	0.3175	0.239444	1.24008027
Average Abs. Deviation:	0.332301375067	0.308584120885	1.38349456648
Quartile Dispersion:	N/A	0.00864917267396	0.0479996595128
Relative Mean Diff.:	N/A	0.0156181417289	0.0737873104995
Standard Error:	0.00908378683246	0.00905025833694	0.0390558604177
Coef. of Variation:	N/A	0.0138209205798	0.0648393425412
Skewness:	-0.104628536194	-0.365873583073	-0.348333992399
Kurtosis:	2.02916661481	2.59258640634	2.61402643808
Sum:	-48193.686686	52232.057514	48046.3871442
Sum Absolute:	48193.686686	52232.057514	48046.3871442
Sum Squares:	1253727.01244	1472589.68347	1251028.14368
Mean Square:	676.593098998	794.705711533	675.136612889

Inter-Variable Covariance

	X	Y	Z
X:	0.15290063	0.064037925	-0.64582942

Y:	0.064037925	0.151774	-0.25944737
Z:	-0.64582942	-0.25944737	2.8264925

Inter-Variable Correlation

	X	Y	Z
X:	1.000	0.420	-0.982
Y:	0.420	1.000	-0.396
Z:	-0.982	-0.396	1.000

Inter-Variable Rank Correlation

	X	Y	Z
X:	1.000	0.415	-0.991
Y:	0.415	1.000	-0.381
Z:	-0.991	-0.381	1.000

Principal Component Analysis

	PC1	PC2	PC3
X:	0.0152601785918	0.0152601785918	0.974860467538
Y:	0.994943533913	0.994943533913	-0.0368768932354
Z:	0.099269790342	0.099269790342	-0.0368768932354
Lambda:	2.99939539303	0.126870014699	0.0049017355195

Planar Regression: Z = AX+BY+C

Fitted Parameters

	A	B	C
Parameter Value:	-4.26085197256	0.088346796403	-87.3795535821
Standard Error:	0.0204751011871	0.0205509553023	0.937319192523

Inter-Parameter Correlations

	A	B	C
A:	1.000	-0.420	0.828
B:	-0.420	1.000	-0.857
C:	0.828	-0.857	1.000

ANOVA Table

Source	df	Sum of Squares	Mean Square	F
Regression:	2	5053.85285616	2526.92642808	
	25854.6591165			
Residual:	1850	180.81127548	0.0977358245836	
Total:	1852	5234.66413164		

Coefficient of Multiple Determination (R^2): 0.965458858308

Nearest Neighbor Statistics

	Separation	|Delta Z|
1%%-tile:	0.000877848506293	0.000338769999999
5%%-tile:	0.00237429673798	0.00293967
10%%-tile:	0.00551315490441	0.00633178
25%%-tile:	0.0108470283949	0.01867463
50%%-tile:	0.0183666330611	0.04696377
75%%-tile:	0.0250078716008	0.08596611
90%%-tile:	0.031760908504	0.11850348
95%%-tile:	0.0353479075477	0.13974688
99%%-tile:	0.0410745633452	0.18009762
Minimum:	0.000620285418175	1.44900000016e-005
Maximum:	0.0586215288269	0.31192717
Mean:	0.0184863563296	0.0563891104965
Median:	0.0183666330611	0.04696377
Geometric Mean:	0.0148154370047	0.0341172367054
Harmonic Mean:	0.00901174885087	0.00424756032957
Root Mean Square:	0.0209132894276	0.0721531610868
Trim Mean (10%%):	0.0182984690008	0.0533175505456
Interquartile Mean:	0.0182122017426	0.0484813902481
Midrange:	0.0296209071225	0.15597083
Winsorized Mean:	0.0183310984343	0.0538572762547
TriMean:	0.0181470415295	0.04964207
Variance:	9.56719351747e-005	0.00202744101201
Standard Deviation:	0.00978120315579	0.0450271141871
Interquartile Range:	0.0141608432058	0.06729148
Range:	0.0580012434087	0.31191268
Mean Difference:	0.0111483903806	0.0496003479861
Median Abs. Deviation:	0.00703342162391	0.03156297
Average Abs. Deviation:	0.00792634274334	0.0362056302536
Quartile Dispersion:	0.394948618112	0.643071522621
Relative Mean Diff.:	0.603060450736	0.879608625662
Standard Error:	0.000227224192984	0.00104601136697
Coef. of Variation:	0.529103895944	0.798507261253
Skewness:	0.229701752614	0.959885784025
Kurtosis:	2.56102245763	4.00158653212

Sum:	34.2552182787	104.48902175
Sum Absolute:	34.2552182787	104.48902175
Sum Squares:	0.81043859519	9.64686374738
Mean Square:	0.000437365674684	0.00520607865482

Complete Spatial Randomness

Lambda:	565.452510436
Clark and Evans:	0.879183206369
Skellam:	2879.36101325

APPENDIX D

Data Statistics Report

Thu May 05 06:02:37 2016

Data Source

Source Data File Name:	C:\Users\Siphiwe\Desktop\Processing-data\comp.Geoid-data\Geoidfftx.dat
X Column:	A
Y Column:	B
Z Column:	C

Data Counts

Active Data:	1853

Original Data:	1853
Excluded Data:	0
Deleted Duplicates:	0
Retained Duplicates:	0
Artificial Data:	0
Superseded Data:	0

Exclusion Filtering

Exclusion Filter String:	Not In Use

Duplicate Filtering

Duplicate Points to Keep:	First
X Duplicate Tolerance:	2E-007
Y Duplicate Tolerance:	2.2E-007

No duplicate data were found.

Breakline Filtering

Breakline Filtering:	Not In Use

Data Counts

Active Data:	1853

Univariate Statistics

	X	Y	Z
Count:	1853	1853	1853
1%%-tile:	-26.777222	27.298889	21.51565851
5%%-tile:	-26.64	27.466389	23.01243913
10%%-tile:	-26.549167	27.592222	23.64518342
25%%-tile:	-26.341667	27.97	24.76368356
50%%-tile:	-25.962778	28.23	25.93593912
75%%-tile:	-25.699167	28.458056	27.26453007
90%%-tile:	-25.507778	28.678333	28.11155604
95%%-tile:	-25.41	28.791944	28.42673036
99%%-tile:	-25.253889	28.923333	28.71316881
Minimum:	-26.903889	27.209167	20.66025888
Maximum:	-25.143889	29.071111	28.90978981
Mean:	-26.0084655618	28.1878346001	25.8919350415
Median:	-25.962778	28.23	25.93593912
Geometric Mean:	N/A	28.1851342443	25.8362938256
Harmonic Mean:	N/A	28.1824242413	25.7795261309
Root Mean Square:	26.0114032493	28.1905252085	25.9464325096
Trim Mean (10%%):	-26.0069829215	28.194846964	25.94145137
Interquartile Mean:	-25.9929342071	28.225078219	25.9629233714
Midrange:	-26.023889	28.140139	24.785024345
Winsorized Mean:	-26.0091646287	28.1894760281	25.9435261972
TriMean:	-25.9915975	28.222014	25.9750229675
Variance:	0.152900634502	0.151773997064	2.8265851933
Standard Deviation:	0.391025107253	0.389581823323	1.68124513183
Interquartile Range:	0.6425	0.488056	2.50084651
Range:	1.76	1.861944	8.24953093
Mean Difference:	0.449728721895	0.440241595816	1.91326270875
Median Abs. Deviation:	0.3175	0.239444	1.23976871
Average Abs. Deviation:	0.332301375067	0.308584120885	1.38352759322
Quartile Dispersion:	N/A	0.00864917267396	0.0480671223461
Relative Mean Diff.:	N/A	0.0156181417289	0.0738941568361
Standard Error:	0.00908378683246	0.00905025833694	0.0390565007397
Coef. of Variation:	N/A	0.0138209205798	0.0649331588827
Skewness:	-0.104628536194	-0.365873583073	-0.348309218253
Kurtosis:	2.02916661481	2.59258640634	2.61402894187
Sum:	-48193.686686	52232.057514	47977.7556319
Sum Absolute:	48193.686686	52232.057514	47977.7556319
Sum Squares:	1253727.01244	1472589.68347	1247471.76804
Mean Square:	676.593098998	794.705711533	673.217359976

Inter-Variable Covariance

	X	Y	Z
X:	0.15290063	0.064037925	-0.64584096
Y:	0.064037925	0.151774	-0.25946328
Z:	-0.64584096	-0.25946328	2.8265852

Inter-Variable Correlation

	X	Y	Z
X:	1.000	0.420	-0.982
Y:	0.420	1.000	-0.396
Z:	-0.982	-0.396	1.000

Inter-Variable Rank Correlation

	X	Y	Z
X:	1.000	0.415	-0.991
Y:	0.415	1.000	-0.381
Z:	-0.991	-0.381	1.000

Principal Component Analysis

	PC1	PC2	PC3
X:	0.015239301107	0.015239301107	0.974861551873
Y:	0.994944103829	0.994944103829	-0.0368557533301
Z:	0.0992672854346	0.0992672854346	-0.0368557533301
Lambda:	2.99949054759	0.126867751785	0.00490152549951

Planar Regression: Z = AX+BY+C

Fitted Parameters

	A	B	C
Parameter Value:	-4.26089032195	0.0882581990165	-87.4150916756
Standard Error:	0.0204748047146	0.0205506577315	0.93730562046

Inter-Parameter Correlations

	A	B	C
A:	1.000	-0.420	0.828
B:	-0.420	1.000	-0.857
C:	0.828	-0.857	1.000

ANOVA Table

Source	df	Sum of Squares	Mean Square	F
Regression:	2	5054.02973865	2527.01486933	25856.3127933
Residual:	1850	180.806039346	0.0977329942412	
Total:	1852	5234.835778		

Coefficient of Multiple Determination (R^2): 0.965460991134

Nearest Neighbor Statistics

	Separation	|Delta Z|
1%%-tile:	0.000877848506293	0.000489269999999
5%%-tile:	0.00237429673798	0.00275889
10%%-tile:	0.00551315490441	0.00623398
25%%-tile:	0.0108470283949	0.01869843
50%%-tile:	0.0183666330611	0.04697098
75%%-tile:	0.0250078716008	0.08592513
90%%-tile:	0.031760908504	0.11849637
95%%-tile:	0.0353479075477	0.13988061
99%%-tile:	0.0410745633452	0.18027117
Minimum:	0.000620285418175	2.58000000031e-006
Maximum:	0.0586215288269	0.31204246
Mean:	0.0184863563296	0.056391202979
Median:	0.0183666330611	0.04697098
Geometric Mean:	0.0148154370047	0.0340642949143
Harmonic Mean:	0.00901174885087	0.00182435950638
Root Mean Square:	0.0209132894276	0.072153583296
Trim Mean (10%%):	0.0182984690008	0.0533213619964
Interquartile Mean:	0.0182122017426	0.0484897468608
Midrange:	0.0296209071225	0.15602252
Winsorized Mean:	0.0183310984343	0.0538522857205
TriMean:	0.0181470415295	0.04964138
Variance:	9.56719351747e-005	0.00202726585429
Standard Deviation:	0.00978120315579	0.0450251691201
Interquartile Range:	0.0141608432058	0.0672267
Range:	0.0580012434087	0.31203988
Mean Difference:	0.0111483903806	0.0496004234445
Median Abs. Deviation:	0.00703342162391	0.03142962
Average Abs. Deviation:	0.00792634274334	0.0362073242957
Quartile Dispersion:	0.394948618112	0.642557947751
Relative Mean Diff.:	0.603060450736	0.879577324551
Standard Error:	0.000227224192984	0.0010459661817
Coef. of Variation:	0.529103895944	0.798443139027
Skewness:	0.229701752614	0.959357170443
Kurtosis:	2.56102245763	4.00016580732
Sum:	34.2552182787	104.49289912

Sum Absolute:	34.2552182787	104.49289912
Sum Squares:	0.81043859519	9.64697664628
Mean Square:	0.000437365674684	0.00520613958245

Complete Spatial Randomness

Lambda:	565.452510436
Clark and Evans:	0.879183206369
Skellam:	2879.36101325

APPENDIX E

Data Statistics Report

Thu May 05 05:58:03 2016

Data Source

Source Data File Name:	C:\Users\Siphiwe\Desktop\Processing-data\comp.Geoid-data\SiPLCS-SiPFFT.dat
X Column:	A
Y Column:	B
Z Column:	C

Data Counts

Active Data:	1853

Original Data:	1853
Excluded Data:	0
Deleted Duplicates:	0
Retained Duplicates:	0
Artificial Data:	0
Superseded Data:	0

Exclusion Filtering

Exclusion Filter String:	Not In Use

Duplicate Filtering

Duplicate Points to Keep:	First
X Duplicate Tolerance:	2E-007
Y Duplicate Tolerance:	2.2E-007

No duplicate data were found.

Breakline Filtering

Breakline Filtering:	Not In Use

Data Counts

Active Data:	1853

Univariate Statistics

	X	Y	Z
Count:	1853	1853	1853
1%%-tile:	-26.777222	27.298889	0.03663165
5%%-tile:	-26.64	27.466389	0.03674629
10%%-tile:	-26.549167	27.592222	0.03681254
25%%-tile:	-26.341667	27.97	0.03691647
50%%-tile:	-25.962778	28.23	0.03703452
75%%-tile:	-25.699167	28.458056	0.03715918
90%%-tile:	-25.507778	28.678333	0.03727304
95%%-tile:	-25.41	28.791944	0.03733428
99%%-tile:	-25.253889	28.923333	0.03741921
Minimum:	-26.903889	27.209167	0.0365136
Maximum:	-25.143889	29.071111	0.03749577
Mean:	-26.0084655618	28.1878346001	0.0370380530383
Median:	-25.962778	28.23	0.03703452
Geometric Mean:	N/A	28.1851342443	0.0370376303123
Harmonic Mean:	N/A	28.1824242413	0.0370372075657
Root Mean Square:	26.0114032493	28.1905252085	0.0370384757424
Trim Mean (10%%):	-26.0069829215	28.194846964	0.0370383339209
Interquartile Mean:	-25.9929342071	28.225078219	0.0370359934304
Midrange:	-26.023889	28.140139	0.037004685
Winsorized Mean:	-26.0091646287	28.1894760281	0.0370390749002
TriMean:	-25.9915975	28.222014	0.0370361725
Variance:	0.152900634502	0.151773997064	3.13293610041e-008
Standard Deviation:	0.391025107253	0.389581823323	0.000177001019783
Interquartile Range:	0.6425	0.488056	0.00024271
Range:	1.76	1.861944	0.00098217
Mean Difference:	0.449728721895	0.440241595816	0.000200902036415
Median Abs. Deviation:	0.3175	0.239444	0.00012014
Average Abs. Deviation:	0.332301375067	0.308584120885	0.000142170966001
Quartile Dispersion:	N/A	0.00864917267396	0.00327651529214
Relative Mean Diff.:	N/A	0.0156181417289	0.0054242061862
Standard Error:	0.00908378683246	0.00905025833694	4.11185753296e-006
Coef. of Variation:	N/A	0.0138209205798	0.00477889643928
Skewness:	-0.104628536194	-0.365873583073	-0.00662367236306
Kurtosis:	2.02916661481	2.59258640634	2.69487477148
Sum:	-48193.686686	52232.057514	68.63151228
Sum Absolute:	48193.686686	52232.057514	68.63151228
Sum Squares:	1253727.01244	1472589.68347	2.5420356139
Mean Square:	676.593098998	794.705711533	0.00137184868532

Inter-Variable Covariance

	X	Y	Z
X:	0.15290063	0.064037925	1.153724e-005

Y:	0.064037925	0.151774	1.5902595e-005
Z:	1.153724e-005	1.5902595e-005	3.1329361e-008

Inter-Variable Correlation

	X	Y	Z
X:	1.000	0.420	0.167
Y:	0.420	1.000	0.231
Z:	0.167	0.231	1.000

Inter-Variable Rank Correlation

	X	Y	Z
X:	1.000	0.415	0.189
Y:	0.415	1.000	0.268
Z:	0.189	0.268	1.000

Principal Component Analysis

	PC1	PC2	PC3
X:	-0.703989952936	-0.703989952936	-3.83493959604e-005
Y:	0.710209930143	0.710209930143	-8.85974031207e-005
Z:	3.59251661914e-005	3.59251661914e-005	-8.85974031207e-005
Lambda:	0.216377720394	0.0882969130234	2.94779861799e-008

Planar Regression: Z = AX+BY+C

Fitted Parameters

	A	B	C
Parameter Value:	3.83493959126e-005	8.85973864216e-005	0.0355380935068
Standard Error:	1.12507817607e-005	1.12924625362e-005	0.000515043788007

Inter-Parameter Correlations

	A	B	C
A:	1.000	-0.420	0.828
B:	-0.420	1.000	-0.857
C:	0.828	-0.857	1.000

ANOVA Table

Source	df	Sum of Squares	Mean Square	F
Regression:	2	3.42874566558e-006	1.71437283279e-006	
	58.0949265607			
Residual:	1850	5.4593230914e-005	2.95098545481e-008	
Total:	1852	5.80219765796e-005		

Coefficient of Multiple Determination (R^2): 0.0590939135084

Nearest Neighbor Statistics

	Separation	|Delta Z|
1%%-tile:	0.000877848506293	1.72e-006
5%%-tile:	0.00237429673798	1.078e-005
10%%-tile:	0.00551315490441	1.95e-005
25%%-tile:	0.0108470283949	4.783e-005
50%%-tile:	0.0183666330611	0.00010917
75%%-tile:	0.0250078716008	0.00024086
90%%-tile:	0.031760908504	0.00035292
95%%-tile:	0.0353479075477	0.00042917
99%%-tile:	0.0410745633452	0.00056204
Minimum:	0.000620285418175	1.29999999994e-007
Maximum:	0.0586215288269	0.00075483
Mean:	0.0184863563296	0.000157961743119
Median:	0.0183666330611	0.00010917
Geometric Mean:	0.0148154370047	9.48543266108e-005
Harmonic Mean:	0.00901174885087	2.43288590319e-005
Root Mean Square:	0.0209132894276	0.000209463146952
Trim Mean (10%%):	0.0182984690008	0.000146548081535
Interquartile Mean:	0.0182122017426	0.000124099320388
Midrange:	0.0296209071225	0.00037748
Winsorized Mean:	0.0183310984343	0.00014891270912
TriMean:	0.0181470415295	0.0001267575
Variance:	9.56719351747e-005	1.8933115189e-008
Standard Deviation:	0.00978120315579	0.000137597656917
Interquartile Range:	0.0141608432058	0.00019303
Range:	0.0580012434087	0.0007547
Mean Difference:	0.0111483903806	0.000148181589973
Median Abs. Deviation:	0.00703342162391	7.752e-005
Average Abs. Deviation:	0.00792634274334	0.000106335261738
Quartile Dispersion:	0.394948618112	0.668641102913
Relative Mean Diff.:	0.603060450736	0.938085305005
Standard Error:	0.000227224192984	3.19648984399e-006
Coef. of Variation:	0.529103895944	0.871082163312
Skewness:	0.229701752614	1.12797776708
Kurtosis:	2.56102245763	3.82025969005

Sum:	34.2552182787	0.29270311
Sum Absolute:	34.2552182787	0.29270311
Sum Squares:	0.81043859519	8.13000228021e-005
Mean Square:	0.000437365674684	4.3874809931e-008

Complete Spatial Randomness

Lambda:	565.452510436
Clark and Evans:	0.879183206369
Skellam:	2879.36101325

APPENDIX F

Data Statistics Report

Fri Apr 29 11:14:46 2016

Data Source

Source Data File Name:	C:\Users\Siphiwe\Desktop\Processing-data\SiPgeoid-egm2008geoid.dat
X Column:	A
Y Column:	B
Z Column:	C

Data Counts

Active Data:	39

Original Data:	39
Excluded Data:	0
Deleted Duplicates:	0
Retained Duplicates:	0
Artificial Data:	0
Superseded Data:	0

Exclusion Filtering

Exclusion Filter String:	Not In Use

Duplicate Filtering

Duplicate Points to Keep:	First
X Duplicate Tolerance:	1.2E-007
Y Duplicate Tolerance:	8E-008

No duplicate data were found.

Breakline Filtering

Breakline Filtering:	Not In Use

Data Counts

Active Data:	39

Univariate Statistics

	X	Y	Z
Count:	39	39	39
1%%-tile:	-26.758333	27.681667	0.133059931
5%%-tile:	-26.735	27.706667	0.146150135
10%%-tile:	-26.686667	27.926667	0.149075595
25%%-tile:	-26.358333	28.078333	0.163420976
50%%-tile:	-25.996667	28.145	0.188949378
75%%-tile:	-25.88	28.223333	0.230478677
90%%-tile:	-25.835	28.236667	0.251227536
95%%-tile:	-25.808333	28.315	0.261474133
99%%-tile:	-25.795	28.33	0.284586427
Minimum:	-26.758333	27.681667	0.133059931
Maximum:	-25.751667	28.356667	0.287822227
Mean:	-26.1259829487	28.1170513333	0.197619421974
Median:	-25.996667	28.145	0.188949378
Geometric Mean:	N/A	28.1166458505	0.193473304363
Harmonic Mean:	N/A	28.116238484	0.18952931851
Root Mean Square:	26.1278000903	28.1174549427	0.20187299968
Trim Mean (10%%):	-26.1280093056	28.1165741111	0.194491357556
Interquartile Mean:	-26.0519167	28.13825	0.1901248748
Midrange:	-26.255	28.019167	0.210441079
Winsorized Mean:	-26.126196641	28.1249573333	0.196027692923
TriMean:	-26.05791675	28.1479165	0.19294960225
Variance:	0.0974512740584	0.0232940555354	0.00174398974417
Standard Deviation:	0.312171866219	0.152623902241	0.0417611032442
Interquartile Range:	0.478333	0.145	0.067057701
Range:	1.006666	0.675	0.154762296
Mean Difference:	0.344862796221	0.160566766532	0.0478257294764
Median Abs. Deviation:	0.15	0.073333	0.032392189
Average Abs. Deviation:	0.245897435897	0.105128205128	0.035146035359
Quartile Dispersion:	N/A	0.00257541224446	0.170240568859
Relative Mean Diff.:	N/A	0.00571065452875	0.242009256978
Standard Error:	0.0499875046075	0.0244393836924	0.00668712836336
Coef. of Variation:	N/A	0.0054281617383	0.211320845021
Skewness:	-0.781667643517	-1.23142895664	0.456005182703
Kurtosis:	2.16248695732	4.47107388678	2.0001305134
Sum:	-1018.913335	1096.565002	7.707157457
Sum Absolute:	1018.913335	1096.565002	7.707157457
Sum Squares:	26623.8155648	30833.0596257	1.589355612
Mean Square:	682.66193756	790.591272453	0.0407527079999

Inter-Variable Covariance

	X	Y	Z
X:	0.097451274	0.040509655	-0.00061096202
Y:	0.040509655	0.023294056	0.0013673629
Z:	-0.00061096202	0.0013673629	0.0017439897

Inter-Variable Correlation

	X	Y	Z
X:	1.000	0.850	-0.047
Y:	0.850	1.000	0.215
Z:	-0.047	0.215	1.000

Inter-Variable Rank Correlation

	X	Y	Z
X:	1.000	0.821	-0.305
Y:	0.821	1.000	-0.023
Z:	-0.305	-0.023	1.000

Principal Component Analysis

	PC1	PC2	PC3
X:	-0.379979933021	-0.379979933021	0.13425951867
Y:	0.862976787454	0.862976787454	-0.304730539257
Z:	0.33299596817	0.33299596817	-0.304730539257
Lambda:	0.115289469823	0.00598474912208	0.00121510039274

Planar Regression: Z = AX+BY+C

Fitted Parameters

	A	B	C
Parameter Value:	-0.110688115489	0.251192854173	-9.75701877125
Standard Error:	0.0370290264712	0.0757379422751	2.99567508402

Inter-Parameter Correlations

	A	B	C
A:	1.000	-0.850	0.927
B:	-0.850	1.000	-0.985
C:	0.927	-0.985	1.000

ANOVA Table

Source	df	Sum of Squares	Mean Square	F
Regression:	2	0.0156217251912	0.00781086259562	5.55166221912
Residual:	36	0.0506498850874	0.00140694125243	
Total:	38	0.0662716102786		

Coefficient of Multiple Determination (R^2): 0.235722734449

Nearest Neighbor Statistics

	Separation	|Delta Z|
1%%-tile:	0.008333	0.000195607
5%%-tile:	0.008333	0.000195607
10%%-tile:	0.013334	0.003085283
25%%-tile:	0.0200692689453	0.005347195
50%%-tile:	0.0310015949428	0.007054254
75%%-tile:	0.035629139142	0.013090204
90%%-tile:	0.0459763465817	0.022935278
95%%-tile:	0.0690010064347	0.03038447
99%%-tile:	0.0698008436768	0.03038447
Minimum:	0.008333	0.000195607
Maximum:	0.0776917985118	0.035465033
Mean:	0.0313537964568	0.011128998641
Median:	0.0310015949428	0.007054254
Geometric Mean:	0.0277276075003	0.00744628845209
Harmonic Mean:	0.0241088362887	0.00252394940551
Root Mean Square:	0.0349856095823	0.0141890673478
Trim Mean (10%%):	0.0296381227674	0.0102218288056
Interquartile Mean:	0.0295439709517	0.00832350405
Midrange:	0.0430123992559	0.01783032
Winsorized Mean:	0.0294919055944	0.0105543527949
TriMean:	0.0294253994933	0.00813647675
Variance:	0.000247272649949	7.95138378032e-005
Standard Deviation:	0.0157249054035	0.00891705320177
Interquartile Range:	0.0155598701967	0.007743009
Range:	0.0693587985118	0.035269426
Mean Difference:	0.0167801892442	0.00955117329015
Median Abs. Deviation:	0.00558935719016	0.003818454
Average Abs. Deviation:	0.01107735344	0.00645325997436
Quartile Dispersion:	0.279359334153	0.419962110708
Relative Mean Diff.:	0.535188434592	0.858223960504
Standard Error:	0.00251800007102	0.00142787126658
Coef. of Variation:	0.501531143929	0.801244881898
Skewness:	1.08513183801	1.07982901343
Kurtosis:	4.25825570806	3.17738791388
Sum:	1.22279806182	0.434030947

Sum Absolute:	1.22279806182	0.434030947
Sum Squares:	0.047735722236	0.00785185565585
Mean Square:	0.00122399287785	0.000201329632201

Complete Spatial Randomness

Lambda:	57.3951814979
Clark and Evans:	0.475070263519
Skellam:	17.2146738797

APPENDIX G

Data Statistics Report

Thu May 05 05:54:02 2016

Data Source

Source Data File Name: C:\Users\Siphiwe\Desktop\Processing-data\comp.Geoid-data\comparing-SAGEOID10\SiPLSC-SAGEOID10.dat
X Column: A
Y Column: B
Z Column: C

Data Counts

Active Data: 1853

Original Data: 1853
Excluded Data: 0
Deleted Duplicates: 0
Retained Duplicates: 0
Artificial Data: 0
Superseded Data: 0

Exclusion Filtering

Exclusion Filter String: Not In Use

Duplicate Filtering

Duplicate Points to Keep: First
X Duplicate Tolerance: 2E-007
Y Duplicate Tolerance: 2.2E-007

No duplicate data were found.

Breakline Filtering

Breakline Filtering: Not In Use

Data Counts

Active Data: 1853

Univariate Statistics

	X	Y	Z
Count:	1853	1853	1853
1%%-tile:	-26.777222	27.298889	-0.19459704
5%%-tile:	-26.64	27.466389	-0.13373703
10%%-tile:	-26.549167	27.592222	-0.110913
25%%-tile:	-26.341667	27.97	-0.07499303
50%%-tile:	-25.962778	28.23	-0.03626168
75%%-tile:	-25.699167	28.458056	-0.00138262
90%%-tile:	-25.507778	28.678333	0.02652389
95%%-tile:	-25.41	28.791944	0.05025309
99%%-tile:	-25.253889	28.923333	0.08425253
Minimum:	-26.903889	27.209167	-0.25354903
Maximum:	-25.143889	29.071111	0.14697278
Mean:	-26.0084655618	28.1878346001	-0.0394267975283
Median:	-25.962778	28.23	-0.03626168
Geometric Mean:	N/A	28.1851342443	N/A
Harmonic Mean:	N/A	28.1824242413	N/A
Root Mean Square:	26.0114032493	28.1905252085	0.0687289533201
Trim Mean (10%%):	-26.0069829215	28.194846964	-0.0385993329137
Interquartile Mean:	-25.9929342071	28.225078219	-0.0373341266559
Midrange:	-26.023889	28.140139	-0.053288125
Winsorized Mean:	-26.0091646287	28.1894760281	-0.0389299829466
TriMean:	-25.9915975	28.222014	-0.0372247525
Variance:	0.152900634502	0.151773997064	0.00317090789043
Standard Deviation:	0.391025107253	0.389581823323	0.0563108150397
Interquartile Range:	0.6425	0.488056	0.07361041
Range:	1.76	1.861944	0.40052181
Mean Difference:	0.449728721895	0.440241595816	0.0628845067335
Median Abs. Deviation:	0.3175	0.239444	0.03703229
Average Abs. Deviation:	0.332301375067	0.308584120885	0.0441806426228
Quartile Dispersion:	N/A	0.00864917267396	N/A
Relative Mean Diff.:	N/A	0.0156181417289	N/A
Standard Error:	0.00908378683246	0.00905025833694	0.00130813963271
Coef. of Variation:	N/A	0.0138209205798	N/A
Skewness:	-0.104628536194	-0.365873583073	-0.289051374815
Kurtosis:	2.02916661481	2.59258640634	3.45596102998
Sum:	-48193.686686	52232.057514	-73.05785582
Sum Absolute:	48193.686686	52232.057514	100.00406856
Sum Squares:	1253727.01244	1472589.68347	8.75295870235
Mean Square:	676.593098998	794.705711533	0.00472366902447

Inter-Variable Covariance

	X	Y	Z
X:	0.15290063	0.064037925	0.00710421

Y:	0.064037925	0.151774	0.0039078196
Z:	0.00710421	0.0039078196	0.0031709079

Inter-Variable Correlation

	X	Y	Z
X:	1.000	0.420	0.323
Y:	0.420	1.000	0.178
Z:	0.323	0.178	1.000

Inter-Variable Rank Correlation

	X	Y	Z
X:	1.000	0.415	0.274
Y:	0.415	1.000	0.122
Z:	0.274	0.122	1.000

Principal Component Analysis

	PC1	PC2	PC3
X:	-0.702627948163	-0.702627948163	-0.044219354028
Y:	0.711083085904	0.711083085904	-0.00719846266401
Z:	-0.025977132289	-0.025977132289	-0.00719846266401
Lambda:	0.216662493932	0.0883547555235	0.00282829000105

Planar Regression: Z = AX+BY+C

Fitted Parameters

	A	B	C
Parameter Value:	0.0433375916345	0.00746221464009	0.877373790002
Standard Error:	0.00348837822648	0.00350130162263	0.159692683937

Inter-Parameter Correlations

	A	B	C
A:	1.000	-0.420	0.828
B:	-0.420	1.000	-0.857
C:	0.828	-0.857	1.000

ANOVA Table

Source	df	Sum of Squares	Mean Square	F
Regression:	2	0.62419871073	0.312099355365	
	110.013015619			
Residual:	1850	5.24832270235	0.00283693119046	
Total:	1852	5.87252141308		

Coefficient of Multiple Determination (R^2): 0.106291432048

Nearest Neighbor Statistics

	Separation	|Delta Z|
1%%-tile:	0.000877848506293	4.962e-005
5%%-tile:	0.00237429673798	0.00033877
10%%-tile:	0.00551315490441	0.00065009
25%%-tile:	0.0108470283949	0.00215412
50%%-tile:	0.0183666330611	0.00554125
75%%-tile:	0.0250078716008	0.0109149
90%%-tile:	0.031760908504	0.01873539
95%%-tile:	0.0353479075477	0.02472768
99%%-tile:	0.0410745633452	0.03874783
Minimum:	0.000620285418175	3.99999999998e-008
Maximum:	0.0586215288269	0.06907283
Mean:	0.0184863563296	0.00805151949811
Median:	0.0183666330611	0.00554125
Geometric Mean:	0.0148154370047	0.00429264650631
Harmonic Mean:	0.00901174885087	6.77542151624e-005
Root Mean Square:	0.0209132894276	0.0115585937929
Trim Mean (10%%):	0.0182984690008	0.00708874819544
Interquartile Mean:	0.0182122017426	0.00582218845739
Midrange:	0.0296209071225	0.034536435
Winsorized Mean:	0.0183310984343	0.00722843445224
TriMean:	0.0181470415295	0.00603788
Variance:	9.56719351747e-005	6.88112592978e-005
Standard Deviation:	0.00978120315579	0.00829525522801
Interquartile Range:	0.0141608432058	0.00876078
Range:	0.0580012434087	0.06907279
Mean Difference:	0.0111483903806	0.00826499244725
Median Abs. Deviation:	0.00703342162391	0.00388628
Average Abs. Deviation:	0.00792634274334	0.00570727574744
Quartile Dispersion:	0.394948618112	0.670347126257
Relative Mean Diff.:	0.603060450736	1.02651337418
Standard Error:	0.000227224192984	0.00019270458294
Coef. of Variation:	0.529103895944	1.03027201635
Skewness:	0.229701752614	1.98333650922
Kurtosis:	2.56102245763	8.46717099078

Sum:	34.2552182787	14.91946563
Sum Absolute:	34.2552182787	14.91946563
Sum Squares:	0.81043859519	0.247562820641
Mean Square:	0.000437365674684	0.00013360109047

Complete Spatial Randomness

Lambda:	565.452510436
Clark and Evans:	0.879183206369
Skellam:	2879.36101325

APPENDIX H

Gridding Report

Thu May 05 05:56:01 2016
Elasped time for gridding: 1.78 seconds

Data Source

Source Data File Name: C:\Users\Siphiwe\Desktop\Processing-data\comp.Geoid-data\comparing-SAGEOID10\SiPFFT-SAGEOID10.dat
X Column: A
Y Column: B
Z Column: C

Data Counts

Active Data: 1853

Original Data: 1853
Excluded Data: 0
Deleted Duplicates: 0
Retained Duplicates: 0
Artificial Data: 0
Superseded Data: 0

Exclusion Filtering

Exclusion Filter String: Not In Use

Duplicate Filtering

Duplicate Points to Keep: First
X Duplicate Tolerance: 2E-007
Y Duplicate Tolerance: 2.2E-007

No duplicate data were found.

Breakline Filtering

Breakline Filtering: Not In Use

Data Counts

Active Data: 1853

Univariate Statistics

	X	Y	Z
Count:	1853	1853	1853
1%%-tile:	-26.777222	27.298889	-0.23153084
5%%-tile:	-26.64	27.466389	-0.17041494
10%%-tile:	-26.549167	27.592222	-0.1479607
25%%-tile:	-26.341667	27.97	-0.11198401
50%%-tile:	-25.962778	28.23	-0.07331947
75%%-tile:	-25.699167	28.458056	-0.03847719
90%%-tile:	-25.507778	28.678333	-0.0104295
95%%-tile:	-25.41	28.791944	0.0132247
99%%-tile:	-25.253889	28.923333	0.04715761
Minimum:	-26.903889	27.209167	-0.29021653
Maximum:	-25.143889	29.071111	0.10998211
Mean:	-26.0084655618	28.1878346001	-0.0764648505666
Median:	-25.962778	28.23	-0.07331947
Geometric Mean:	N/A	28.1851342443	N/A
Harmonic Mean:	N/A	28.1824242413	N/A
Root Mean Square:	26.0114032493	28.1905252085	0.0949465134983
Trim Mean (10%%):	-26.0069829215	28.194846964	-0.0756469210731
Interquartile Mean:	-25.9929342071	28.225078219	-0.0743875322654
Midrange:	-26.023889	28.140139	-0.09011721
Winsorized Mean:	-26.0091646287	28.1894760281	-0.0759702997302
TriMean:	-25.9915975	28.222014	-0.074275035
Variance:	0.152900634502	0.151773997064	0.00316967761867
Standard Deviation:	0.391025107253	0.389581823323	0.0562998900414
Interquartile Range:	0.6425	0.488056	0.07350682
Range:	1.76	1.861944	0.40019864
Mean Difference:	0.449728721895	0.440241595816	0.0628741199758
Median Abs. Deviation:	0.3175	0.239444	0.03695125
Average Abs. Deviation:	0.332301375067	0.308584120885	0.0441686812574
Quartile Dispersion:	N/A	0.00864917267396	N/A
Relative Mean Diff.:	N/A	0.0156181417289	N/A
Standard Error:	0.00908378683246	0.00905025833694	0.00130788583736
Coef. of Variation:	N/A	0.0138209205798	N/A
Skewness:	-0.104628536193	-0.365873583074	-0.286625176304
Kurtosis:	2.02916661481	2.59258640634	3.45338876474
Sum:	-48193.686686	52232.057514	-141.6893681
Sum Absolute:	48193.686686	52232.057514	148.91539368
Sum Squares:	1253727.01244	1472589.68347	16.7044993084
Mean Square:	676.593098998	794.705711533	0.00901484042549

Inter-Variable Covariance

	X	Y	Z
X:	0.15290063	0.064037925	0.0070926728
Y:	0.064037925	0.151774	0.003891917
Z:	0.0070926728	0.003891917	0.0031696776

Inter-Variable Correlation

	X	Y	Z
X:	1.000	0.420	0.322
Y:	0.420	1.000	0.177
Z:	0.322	0.177	1.000

Inter-Variable Rank Correlation

	X	Y	Z
X:	1.000	0.415	0.274
Y:	0.415	1.000	0.122
Z:	0.274	0.122	1.000

Principal Component Analysis

	PC1	PC2	PC3
X:	-0.702628451442	-0.702628451442	-0.0441811466737
Y:	0.7110812255	0.7110812255	-0.00710829097939
Z:	-0.0260144184185	-0.0260144184185	-0.00710829097939
Lambda:	0.216661079676	0.0883549211515	0.00282830835702

Planar Regression: Z = AX+BY+C

Fitted Parameters

	A	B	C
Parameter Value:	0.0432992422386	0.00737361725366	0.841835696496
Standard Error:	0.00348838143091	0.00350130483893	0.159692830631

Inter-Parameter Correlations

	A	B	C

A:	1.000	-0.420	0.828
B:	-0.420	1.000	-0.857
C:	0.828	-0.857	1.000

ANOVA Table

Source	df	Sum of Squares	Mean Square	F
Regression:	2 109.609542999	0.621910605186	0.310955302593	
Residual:	1850	5.24833234459	0.00283693640248	
Total:	1852	5.87024294978		

Coefficient of Multiple Determination (R^2): 0.10594290739

Nearest Neighbor Statistics

	Separation	|Delta Z|
1%%-tile:	0.000877848506293	7.77e-005
5%%-tile:	0.00237429673798	0.0003609
10%%-tile:	0.00551315490441	0.00069657
25%%-tile:	0.0108470283949	0.00216072
50%%-tile:	0.0183666330611	0.00554819
75%%-tile:	0.0250078716008	0.01092087
90%%-tile:	0.031760908504	0.01877543
95%%-tile:	0.0353479075477	0.02447345
99%%-tile:	0.0410745633452	0.038738
Minimum:	0.000620285418175	6.11e-006
Maximum:	0.0586215288269	0.06895754
Mean:	0.0184863563296	0.00806411204533
Median:	0.0183666330611	0.00554819
Geometric Mean:	0.0148154370047	0.00435409089594
Harmonic Mean:	0.00901174885087	0.00094144370357
Root Mean Square:	0.0209132894276	0.0115667192834
Trim Mean (10%%):	0.0182984690008	0.00710260948441
Interquartile Mean:	0.0182122017426	0.00583533744337
Midrange:	0.0296209071225	0.034481825
Winsorized Mean:	0.0183310984343	0.00724833623314
TriMean:	0.0181470415295	0.0060444925
Variance:	9.56719351747e-005	6.87962188403e-005
Standard Deviation:	0.00978120315579	0.00829434860856
Interquartile Range:	0.0141608432058	0.00876015
Range:	0.0580012434087	0.06895143
Mean Difference:	0.0111483903806	0.00826857023762
Median Abs. Deviation:	0.00703342162391	0.00388022
Average Abs. Deviation:	0.00792634274334	0.0057144827469
Quartile Dispersion:	0.394948618112	0.669654835536
Relative Mean Diff.:	0.603060450736	1.02535408624

Standard Error:	0.000227224192984	0.000192683521535
Coef. of Variation:	0.529103895944	1.02855076442
Skewness:	0.229701752614	1.9780172244
Kurtosis:	2.56102245763	8.43771912598
Sum:	34.2552182787	14.94279962
Sum Absolute:	34.2552182787	14.94279962
Sum Squares:	0.81043859519	0.247911007699
Mean Square:	0.000437365674684	0.000133788994981

Complete Spatial Randomness

Lambda:	565.452510436
Clark and Evans:	0.879183206369
Skellam:	2879.36101325

Gridding Rules

Gridding Method:	Kriging
Kriging Type:	Point
Polynomial Drift Order:	0
Kriging std. deviation grid:	no

Semi-Variogram Model

Component Type:	Linear
Anisotropy Angle:	0
Anisotropy Ratio:	1
Variogram Slope:	1

Search Parameters

Search Ellipse Radius #1:	1.28
Search Ellipse Radius #2:	1.28
Search Ellipse Angle:	0
Number of Search Sectors:	4
Maximum Data Per Sector:	16
Maximum Empty Sectors:	3
Minimum Data:	8
Maximum Data:	64

Output Grid

Grid File Name:	C:\Users\Siphiwe\Desktop\Processing-data\comp.Geoid-data\comparing-SAGEOID10\SiPFFT-SAGEOID10.grd
Grid Size:	100 rows x 95 columns
Total Nodes:	9500
Filled Nodes:	9500
Blanked Nodes:	0
Blank Value:	1.70141E+038

Grid Geometry

X Minimum:	-26.903889
X Maximum:	-25.143889

X Spacing:	0.018723404255319
Y Minimum:	27.209167
Y Maximum:	29.071111
Y Spacing:	0.018807515151515

Univariate Grid Statistics

	Z
Count:	9500
1%%-tile:	-0.225802653545
5%%-tile:	-0.17954220525
10%%-tile:	-0.162555866852
25%%-tile:	-0.130904769937
50%%-tile:	-0.0947027358238
75%%-tile:	-0.0514506883169
90%%-tile:	-0.0037138679617
95%%-tile:	0.0239386531884
99%%-tile:	0.0812160283915
Minimum:	-0.287157363946
Maximum:	0.111957455973
Mean:	-0.0891118321587
Median:	-0.0947020382527
Geometric Mean:	N/A
Harmonic Mean:	N/A
Root Mean Square:	0.108933437615
Trim Mean (10%%):	-0.0906934711523
Interquartile Mean:	-0.0937467132263
Midrange:	-0.0875999539864
Winsorized Mean:	-0.0902106206547
TriMean:	-0.0929402324754
Variance:	0.0039259884619
Standard Deviation:	0.0626577087188
Interquartile Range:	0.07945408162
Range:	0.39911481992
Mean Difference:	0.0699216290763
Median Abs. Deviation:	0.0394853590962
Average Abs. Deviation:	0.0490297639686
Quartile Dispersion:	N/A
Relative Mean Diff.:	N/A
Standard Error:	0.000642854527368
Coef. of Variation:	N/A
Skewness:	0.393098265798
Kurtosis:	3.30781291205
Sum:	-846.562405508
Sum Absolute:	909.298240365
Sum Squares:	112.731691391
Mean Square:	0.0118664938306